

Special issue: Materials for waste and biomass combustion

**Materials performance in simulated
waste combustion environments** page 2

**High temperature corrosion
under simulated biomass deposit
conditions** page 9

**Stainless steels in waste and biomass
power plant applications** page 18



Combustion of waste and biomass is making an increasing contribution to sustainable energy production. However, the very corrosive conditions limit plant efficiency and component lifetimes.

The present three articles describe how stainless steels make attractive alternatives to low-alloyed steels in boilers, and can be the material of choice in flue gas cleaning systems.

Materials performance in simulated waste combustion environments

Rachel Pettersson, Swerea KIMAB AB, Sweden (now at Outokumpu Stainless AB, Sweden)

Jesper Flyg, Swerea KIMAB AB, Sweden

Peter Viklund, Swerea KIMAB AB, Sweden

Abstract

Combustion of waste for power generation gives increased fouling and corrosion compared to fossil fuels, and leads to higher operating and maintenance costs. New materials solutions to increase lifetime include austenitic stainless steels, nickel-base alloys, coatings and weld overlaying.

In this work a simulated waste incineration environment with regularly renewed deposits of KCl-ZnCl₂ has been used to evaluate the performance of candidate materials and to elucidate the operative degradation mechanisms.

Keywords: high temperature corrosion, chloride, deposits, power generation

Introduction

The combustion of waste is making an increasing contribution to environmental maintenance, by reducing the amount of dumped waste, and to the production of “green” electricity from renewable sources. However, operation of waste combustion plants is hampered by the occurrence of severe corrosion problems. This means that the operating conditions must be limited to relatively low temperatures, which correspondingly limit the plant efficiency.

Corrosion problems occur in most stages of the combustion process, from the grate and waterwalls to the superheaters, flue gas cleaning systems and flue gas ducts. Fluidised bed systems also show corrosion in many areas, exacerbated by the occurrence of erosion. In the majority of cases the principal corrosive element is chlorine, present as HCl or metal chlorides. Mixed chloride systems containing heavy metals are particularly damaging, since these often have a low melting point. This gives rise to a melted or partially melted salt deposit which can drastically increase the rate of corrosion [1, 2]. In order to simulate this situation in laboratory testing, a deposit of 50 molar percent KCl and 50 molar percent ZnCl₂ is employed in this study. This forms a low melting point eutectic which has been used in various published studies [2, 3] to induce corrosion in laboratory tests

Experimental

Laboratory testing was performed in a simulated waste combustion superheater environment at 320°C and 420°C. The materials tested were carbon steel EN 1.0570, two different heats of stainless steel EN 1.4307 or 304L (18Cr-8Ni-7Mn-0.4Si by weight percent). These are hereafter denoted 304-1 and 304-2. In addition, nickel-base weld specimen were produced by making two MAG weld overlay passes on carbon steel using Inconel 625 electrodes with a composition of Ni-22Cr-9Mo. The total weld thickness was 6–7 mm and specimens were taken from the outer region where the iron content from incorporation of the base metal was below 10%. Test specimens had dimensions of approximately 16 x 12 x 3 mm, with the exception of 304-1 where the specimens were only 10 x 10 x 1.5 mm. All specimens were wet surface ground to 600 grit SiC before testing, then measured in at eight different positions along the centrelines to an accuracy equal to or better than ± 2µm using a calibrated micrometer, ultrasonically cleaned in acetone rinsed in ethanol and weighed.

The test environment was 0.2% HCl + 0.02% SO₂ + 8% O₂ + 15% H₂O with the

balance as nitrogen. This is an environment which has been established within the PREWIN European network on performance, reliability and emissions reductions in waste incinerators. The gas flow rate during testing was $150 \text{ ml}\cdot\text{min}^{-1}$, which corresponded to a flow rate past the specimens of $4.3 \text{ mm}\cdot\text{s}^{-1}$. A deposit corresponding to $\sim 0.8 \text{ mg}\cdot\text{cm}^{-2}$ dry salt of composition 50 molar percent ZnCl_2 + 50 molar percent KCl was applied to the specimens prior to testing by dipping in aqueous solution. The salt loading was determined by weighing of the wet specimens, since adequate drying could not be achieved at moderate temperatures. Calculation with the SALT1 database in ThermoCalc [4] indicate that molten phases exist in this system down to a temperature of 154°C .

Specimens were placed in individual alumina crucibles to allow collection of spall, and inclined at an angle to minimise contact with the crucible. The test sequence involved exposure for 160 hours at the test temperature, cooling to ambient temperature, weighing, renewal of the deposit, then replacement in the furnace for the following cycle. A total of 14 exposure cycles were carried out at 320°C and 12 cycles at 420°C .

After testing, specimens were wrapped in foil to retain as much as possible of the corrosion products then mounted in clear plastic and sectioned along the long axis. For post test metallography the long sides of the specimen were divided into eight sections of approximately equal size. Each section was examined at $320\times$ magnification in order to locate the area with smallest remaining metal thickness, m , where measurements were made. This area was then examined at $1620\times$ magnification so that a length of surface of $100\mu\text{m}$ could be viewed in a single field and the thickness of remaining metal evaluated using a digital travelling stage. The metal loss was evaluated as

$$P = \frac{t-m}{2}$$

where t is thickness of the specimen measured for that position in the pre-test metrology and m is the remaining metal thickness.

This procedure meant that the entire cross section length was examined and each chosen field contained a local minimum in the remaining metal thickness which could be related to a reference point from the pre-test metrology. Manual selection of measurement points in this manner meant that the potential disadvantage with automatic measurements, i.e. that the most severe corrosion attack lay between measurement points, was avoided.

Results and discussion

Corrosion rates and metal loss

The net mass change curves at the two temperatures, Figure 1, showed a relatively stable behaviour. The carbon steel at 320°C exhibited a successive mass loss which amounted to $30 \text{ mg}\cdot\text{cm}^{-2}$, at the end of testing, but in the other cases the changes were below $10 \text{ mg}\cdot\text{cm}^{-2}$. This is on the same scale as the amount of applied deposit, which was $0.8 \text{ mg}\cdot\text{cm}^{-2}$ per

Fig. 1 Net mass change curves during exposure in the simulated waste combustion environment. The total mass of deposit applied was $\sim 10 \text{ mg}\cdot\text{cm}^{-2}$ during the course of testing.

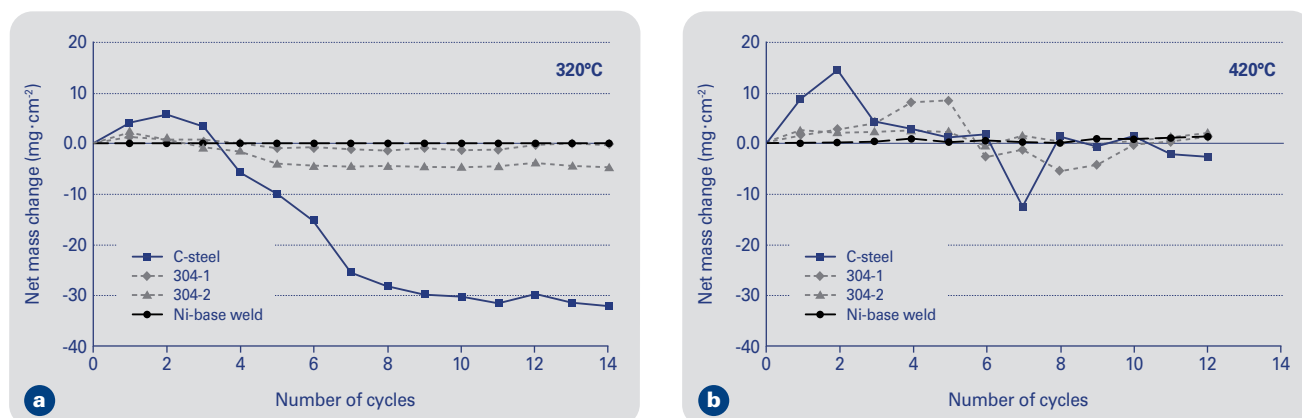
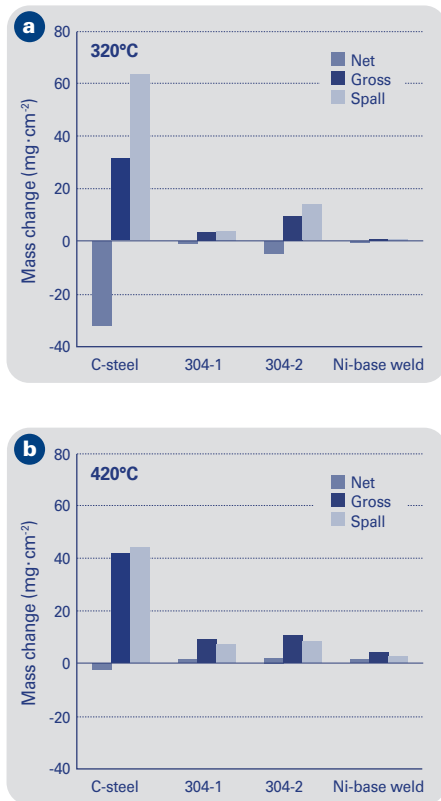


Fig. 2 Comparison between net and gross mass changes at the conclusion of testing. The amount of spall is the difference between the two.



cycle, making a total of approximately 10 mg·cm⁻² over the duration of the test. The net mass change can, however, easily be misleading since it includes several factors which counteract each other: a mass gain due to deposition and oxidation and a mass loss due to spallation and volatilisation of applied salts or metal chlorides.

The gross mass change, which includes both the mass of the specimen and the spalled corrosion products, is a somewhat more useful measure. Data at the conclusion of testing are given in Figure 2, and show slightly higher mass gains for all materials at 420°C than at 320°C. There is also clear differentiation between the materials. The carbon steel exhibited mass changes of over 30 mg·cm⁻². For the 304L stainless steels the figures were below 10 mg·cm⁻² while those for the nickel base overlay weld were 0.5 mg·cm⁻² at 320°C and 4 mg·cm⁻² at 420°C. Two factors mean that even the gross mass changes may be a relatively poor measure of materials performance. One is the occurrence of volatilisation, which causes a mass loss but is not possible to measure when performing testing on multiple specimens. Volatilisation may involve evaporation of the salt deposit or the formation of new volatile species such as metal chlorides or oxyhydroxides [5]. The gross mass increases for the nickel base weld are significantly lower than the total amount of applied salt, so some loss to vaporisation has undoubtedly occurred.

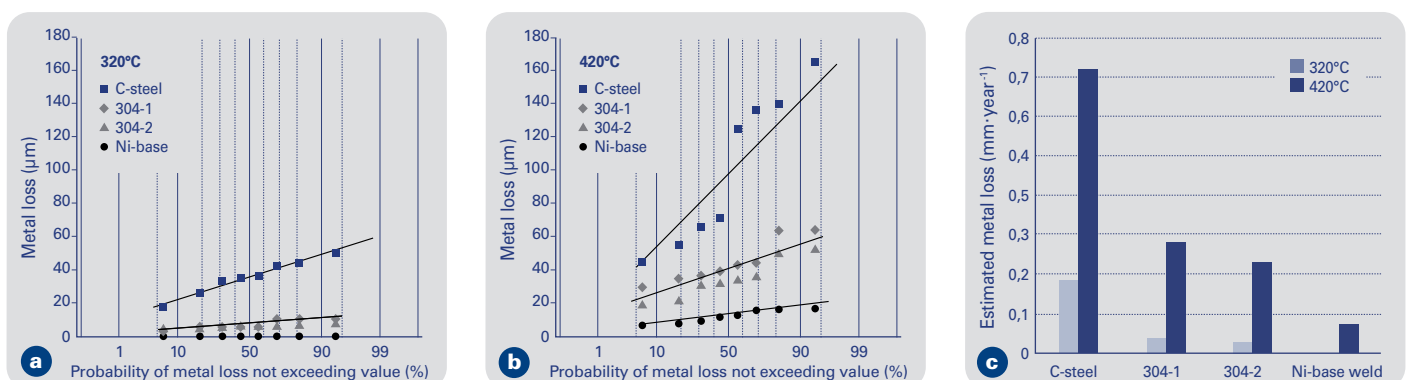
The other factor to be taken into account when judging the amount of materials damage is the morphology of attack. Formation of a fine network of internal oxides or other corrosion products can render a component structurally unsound even though the total mass change is small. For this reason the use of metrology to assess the actual material damage is a vital part of materials evaluation in corrosion studies.

The results of measurements on cross sections are shown in Figure 3. At 320°C the metal loss followed a normal distribution and there was no significant difference between the two heats of 304L investigated. At 420°C the carbon steel exhibited quite a high degree of scatter which could be regarded as a bimodal distribution and the two 304L variants showed slight differences. The metal loss for the nickel-base weld overlay was not measurable at 320°C; where corrosion was only apparent as a slight discoloration of the surface, but some attack was seen at 420°C.

The corrosion product layers were relatively compact, as illustrated by the micrographs in Figure 4. Consequently, there is also quite good agreement between the gross mass change and the measured metal loss, with the same trends in both cases. The measured metal loss in Figure 3 can be used to estimate metal wastage rates if kinetics are known. The worst-case assumption is that the metal loss is linear, which seems reasonable in view of the non-protective nature of the corrosion products and the often large amount of spallation. This gives wastage rates of 0.7 mm per year for carbon steel at 420°C and 0.2 mm per year at 320°C. Corresponding values for 304L are 0.3 and 0.04 mm per year respectively, while the nickel base overlay weld at 420°C would lose 0.07 mm per year.

This indicates that if carbon steel is replaced by 304L austenitic stainless steel, the temperature can be increased from 320°C to 420°C with only marginal increase in corrosion rate. Replacement of 304L by the nickel-base overlay weld has a similar effect.

Fig. 3 Probability plots for metal penetration and maximum measured metal penetration after 14 cycles (2240 hours) at 320°C or 12 cycles (1920 hours) at 420°C.

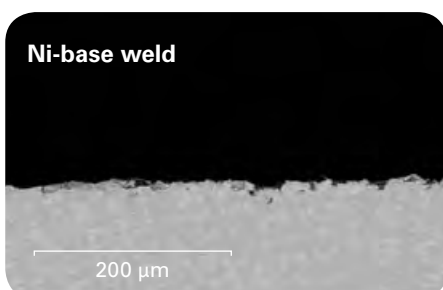
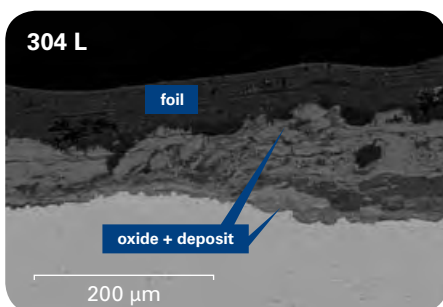
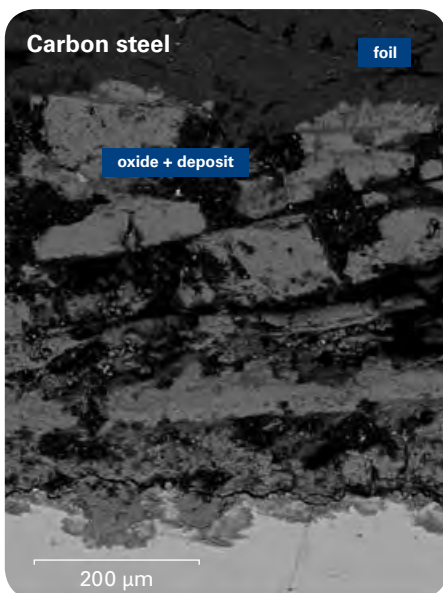


Caution must naturally be exercised in applying this data to the more complex situation in a waste combustion plant, but the results nevertheless indicate the potential gains from the use of more advanced materials.

There is a continual drive towards higher steam temperatures in order to improve the electricity production efficiency in WTE (waste-to-energy) plants. The total efficiency is difficult to predict, since it depends on such factors as the number of reheat steps, pumping systems etc. However, a rough estimate of the potential energy gains attainable may be obtained from the theoretical maximum efficiency in a Carnot cycle. This efficiency, η , depends only on the highest and lowest temperatures, T_{\max} och T_{\min} , according to the relation:

$$\eta = 1 - \left(\frac{T_{\min}}{T_{\max}} \right)$$

Fig. 4 Corrosion products on the three materials after testing for 12 cycles in the simulated waste combustion environment at 420°C. A foil has been used to retain the corrosion products for sectioning.



Corrosion mechanisms

The carbon steel showed extensive spallation at 320°C but retained most of the corrosion products after testing at 420°C. These comprised alternating or irregular layers of salt deposits and oxides, as shown in Figure 5. The most interesting aspect of the deposit was that although the specimens were recoated each cycle with KCl and ZnCl₂, the deposit after testing at 420°C contained predominantly sulphur with less than 1% chlorine. The oxygen content of the deposit suggests that it comprises mainly potassium and zinc sulphates. The zinc content was highest in the outer layers of the deposits, and was partially replaced by iron at greater depth, while the potassium content showed less variation. Thermodynamic calculations, Figure 6a, based on the gas composition used in this investigation support the observation of sulphates in that SO₂ is predicted to convert to sulphates over a range of oxygen partial pressures.

The only location where appreciable levels of chlorine were observed was at the metal-oxide interface, where up to 40% Cl was seen together with 50% Fe and 10% O. All elemental compositions are given in weight percent unless stated otherwise.

Fig. 5 Carbon steel exposed in the high temperature waste environment (420°C), showing extensive corrosion with alternating deposit and oxide layers. Cl was concentrated at the base of the corrosion layer at levels of up to 40 weight percent but was present in concentrations of <1% otherwise.

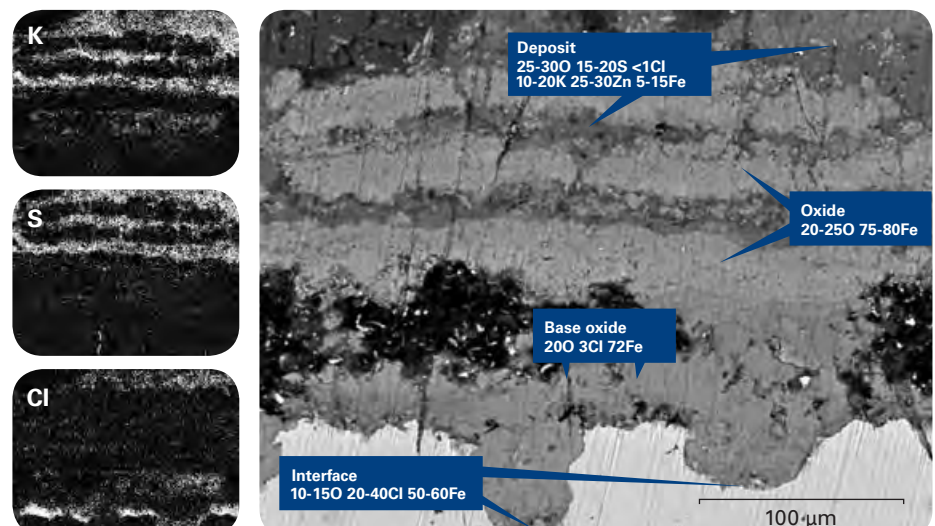
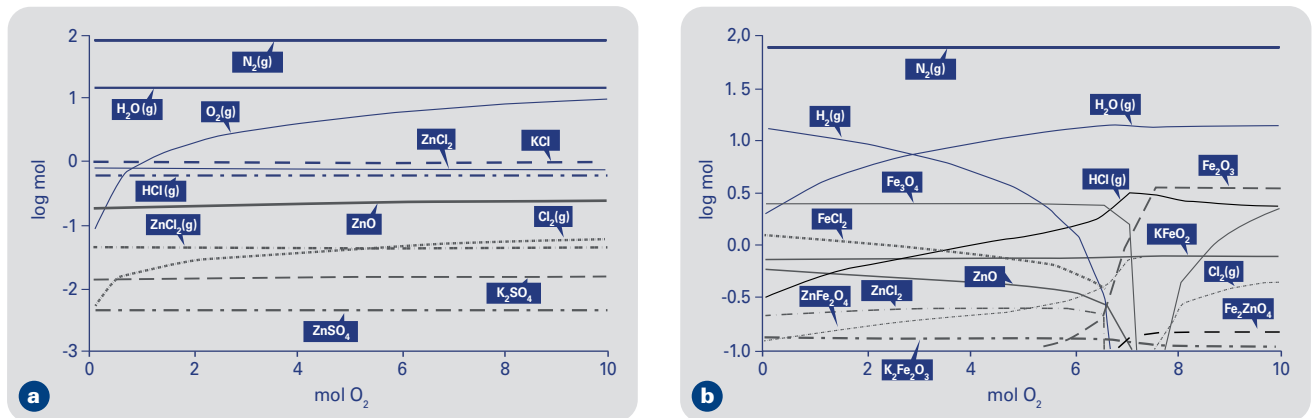


Fig. 6 Calculation of equilibrium components as a function of oxygen level at 420°C using HSC 4.1 [11] database with suspension of wüstite.

(a) 77 mol N_2 , 15 mol H_2O , 0.2 mol HCl , 0.02 mol SO_2 , 1 mol $ZnCl_2$ and 1 mol KCl showing conversion of SO_2 to sulphates.

(b) The same but with addition of 10 mol Fe showing stability of $FeCl_2$ and $HCl(g)$ as chlorine-containing species.



This is in reasonable agreement with the thermodynamic calculations in Figure 6b and observations in other works [6, 7] of the presence of $FeCl_2$ at low oxygen partial pressures. Even though particular care was taken, with dry specimen preparation immediately before examination in the SEM, iron chlorides are deliquescent and rapidly pick up moisture from the atmosphere. This is the most probable reason for the observed oxygen level. The role of this $FeCl_2$ is debated in the literature. One suggestion is the “active oxidation” concept in which volatilisation of $FeCl_2$ and its regeneration as Cl_2 plays a key role [8, 9, 10]. Another is that of “chloride catalysed oxidation” [7] in which the $FeCl_2$ has a catalytic function and only minor transport of chloride-bearing species, primarily HCl , is required. The current observation tend to support the latter since the calculations in Figure 6 predict HCl rather than Cl_2 to dominate at low oxygen partial pressures.

The corrosion layers formed on 304L at 420°C, Figure 7 showed both similarities and differences compared to the carbon steel. There was a similar layered structure comprising potassium-zinc sulphates with an increasing iron content and decreasing zinc content

Fig. 7 Two different areas on the same 304L specimen after exposure in simulated waste combustion environment at 420°C. Corrosion products show alternating layers of deposit and oxides with some nickel sulphides. Chlorine is relatively evenly distributed through the oxide at concentrations around 1–3 weight percent.

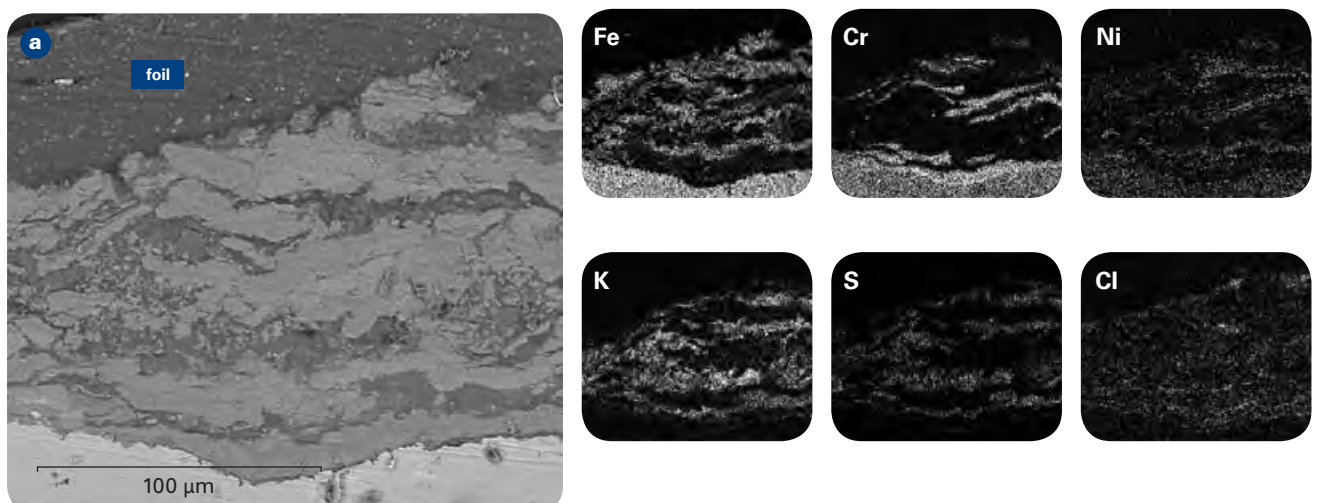
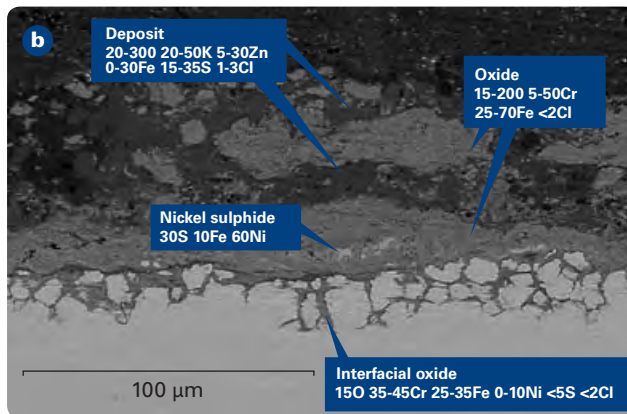


Fig. 7b Corrosion products on 304L after exposure in the simulated waste combustion environment at 420°C.



with depth from the outer surface. This was interleaved with layers of oxide with widely variable levels of iron and chromium. The most significant difference was that chlorine was only present at relatively low levels of 1–3% within the scale, and there was no concentration of chlorine at the metal-oxide interface. Instead the oxide in contact with the metal was strongly enriched in chromium. This suggests that the role of chromium alloying in reducing the corrosion rate of 304L compared to carbon steel is to form an oxide at the low oxygen partial pressures prevalent at the oxide metal interface. This will reduce the iron activity and thus suppress the formation of FeCl_2 .

At the lower test temperature of 320°C there was a thinner and more compact corrosion product layer on 304L, Figure 8. This had a variable composition but no clear structure and again only low levels of chlorine, below 5%.

Both zinc and potassium contents dropped with increasing depth from the outer surface, but there was less pronounced enrichment of chromium at the oxide-metal interface than was seen at 420°C. Slower diffusion both in the metal and in the compact scale, also reduced reaction rates have undoubtedly contributed to the lower metal loss seen at 320°C.

For the nickel-base overlay weld, the amount of corrosion was very limited. At 320°C corrosion gave only a slight surface discoloration on which the original grinding marks were still visible. At 420°C the metal loss was measured as 17 μm, Figure 3, and this is also seen from the surface roughness in Figure 9. Only very small pockets of oxide, containing some sulphide and chloride, were retained on the surface. Sulphidation of the deposit by reaction with the gas atmosphere, which was very clear for the carbon steel, also occurred for the nickel-base overlay weld. However, there was no indication of nickel sulphide formation. This generally becomes more of a problem at higher temperatures, where the nickel-nickel sulphide eutectic melting at 635°C can form.

Fig. 8 304L exposed at the lower temperature of 320°C for 14 cycles. In this case there was a single oxide/deposit layer with variable composition and relatively low levels of sulphur and chlorine.

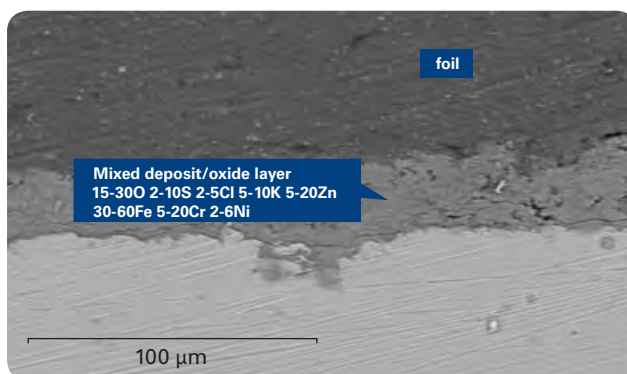
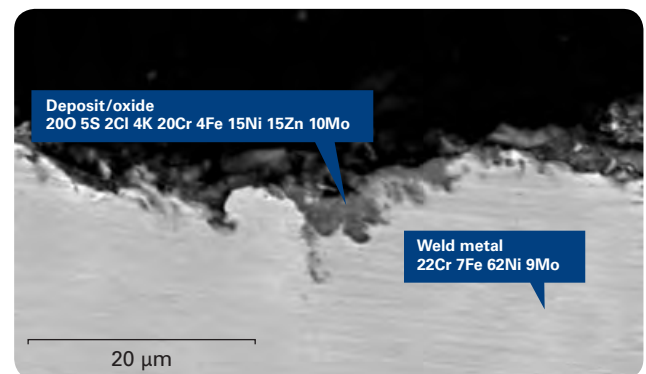


Fig. 9 Small areas of deposit/oxide present on weld overlay exposed at 420°C for 12 cycles.



Conclusions

Evaluation of corrosion rates in a simulated waste incineration environment have indicated that appreciable benefits in terms of reduced materials wastage rates can be achieved by replacement of carbon steel by 304L, or by overlay welding with a nickel base filler. This can offset the increase in corrosion rate resulting from a temperature increase from 320°C to 420°C.

The eutectic KCl-ZnCl₂ deposit was applied every 160 hours throughout the test period of 1920–2240 hours, but was largely converted to sulphates as a result of reaction with the test gas N₂-15%O₂-8%O₂-0.2%HCl-0.02%SO₂. The high corrosion rate on carbon steel was associated with formation of a thin iron chloride layer at the metal-oxide interface. In 304L, a chromium-rich oxide formed at this location, reducing the iron activity and suppressing iron chloride formation.

Acknowledgements

This research project was carried out with a financial grant from the Research Fund for Coal and Steel of the European Community under contract no. RFS-CR-03020. Thanks are also expressed to Fundacion INASMET for provision of the weld overlay samples.

References

- [1] Y. Kawahara: Corrosion Science 44 (2002) 223–245
- [2] M. Spiegel Proc Conf. NACE Corrosion 99 Paper 337
- [3] M. Spiegel: Proc Conf. Eurocorr '99
- [4] B. Sundman, B. Jansson, J.-O. Andersson Calphad 9 (1985) 153
- [5] B.B.Ebbinghaus Combustion and Flame 93(1993) 119–137
- [6] H. J. Grabke, E. Reese, M. Spiegel: Corrosion Science 37:7 (1995) 1023–1043
- [7] P. Szakálos, P. Henderson, R. Pettersson: Proc. 16th International Corrosion Conf. Beijing (Sept 2005)
- [8] Y. Y. Lee, M. J. McNallan. Metallurgical Transactions 18A (1987) 1099–1107
- [9] H. J. Grabke. Proc Incinerating Municipal and Industrial Waste. Hemisphere Publ. Corp (1991) 161–176
- [10] M. Spiegel Materials at high temperatures 14:3 (1997) 221–226
- [11] HSC Chemistry v 4.1 Outokumpu Research Oy, Finland

High temperature corrosion under simulated biomass deposit conditions

Rachel Pettersson, Outokumpu Stainless AB, Sweden

Jesper Flyg and Peter Viklund, Swerea KIMAB AB, Sweden

Abstract

Biomass is gaining increasing importance as a renewable energy source for the production of heat, electricity and transport fuels. However, corrosion issues are numerous and include accelerated wastage under ash and alkali salt deposits, erosion, and metal dusting in conjunction with gasification.

This work focuses on deposit issues and is based on laboratory exposures for a total of 960 hours at 550°C (1022°F) and 700°C (1292°F) under deposits of 52.4 weight percent KCl + 47.6 weight percent K₂SO₄ in a nitrogen-based gaseous atmosphere containing 15% H₂O, 5% O₂, 13% CO₂ and 0.02% HCl.

The materials tested include carbon steel, low-alloyed 2Cr or 9Cr ferritic steels, the austenitic AISI 304 and the high temperature grade 253MA[®] (21Cr-11Ni-1.6Si-Ce). Metal loss data obtained from metallographic evaluation show the corrosion rate to decrease in this order and illustrate how materials substitution can permit an increase in process temperature. Examination of the reaction interface underlines the importance of both chlorination and oxidation in the materials corrosion process.

Keywords: high temperature corrosion, deposits, power generation

Introduction

The production of electricity in biomass fired boilers is increasing rapidly due to the dual advantages of renewability and CO₂ neutrality. However, corrosion and fouling of superheater tubes is a serious concern in these plants and limits the steam temperature and thus the efficiency of the turbine. Corrosion can also lead to unplanned plant stoppages due to tube rupture.

Wood-based fuels typically have high contents of potassium and chlorine. The high corrosivity of the gas environment is usually attributed to the presence of chlorides in the fuel, which are released during combustion and transported by the flue gas to the superheater tubes. These deposited chlorides cause premature failure of normally protective or semi-protective oxides on superheater alloys. The dominant theory for the detrimental effect of chlorides on high temperature corrosion in oxidizing atmospheres is the “active oxidation” or chloride-catalysed oxidation process [1, 2, 3, 4]. This is thought to involve formation of volatile metal chlorides which can oxidise to re-release Cl₂ which again reacts with the metal to form more volatile chlorides. Some work has indicated that Cl₂ is needed from the beginning and that HCl does not take part in the chlorine induced active corrosion, [5, 6], others suggest that it is HCl which plays a critical role in maintaining a catalytic molten chloride at the oxide-metal interface [6]. The deposits on the superheaters normally involve both a solid ash phase and a molten salt phase, and the presence of a liquid on the surface of a metal strongly increases corrosion rates [7, 8]. The alkali metal potassium has also been proposed to play an active role in the corrosion process, and it has been demonstrated that potassium salts can react with otherwise protective chromium oxides to form non-protective potassium chromates, which can lead to the initiation of a corrosion process [9].

The present work involves testing in a simulated biomass combustion environment, with HCl present in the gas phase and a regularly renewed deposit of $\text{KCl} + \text{K}_2\text{SO}_4$. This type of testing is a useful complement to field tests in boilers, since it allows exact control of deposition amounts and gas flow rates.

Experimental

The materials investigated included carbon steel, a 2Cr-1Mo steel (UNS K21950) a 9Cr steel (UNS K51960) two different heats of 304L (UNS 30403) and the high temperature stainless steel 253 MA[®], (21Cr-11Ni-1.6Si-Ce, UNS S30815). The latter was available both as 3 mm sheet from Outokumpu Stainless and as \varnothing 88 x 6 mm seamless tube provided by Sandvik Materials Technology. The compositions of the stainless steels investigated are given in Table 1.

Compositions of the alloys investigated. All values are given in weight percent.

Table 1

UNS	EN	C	Si	Mn	Cr	Ni	Mo	N	Other
K21590	1.7380	0.12	0.2	0.4	2.1		0.9		
K91560	1.4903		0.4	0.4	9	0.4	1		V
S30403	1.4307	0.02	0.3	1.7	18.2	8.4	0.4	0.07	
S30815	1.4835	0.09	1.6	0.6	21.0	10.9	0.2	0.17	Ce

For the laboratory exposures, test specimens of approximate dimensions 16 x 12 x 3 mm were employed. These were wet surface ground to 600 grit SiC before testing and placed in individual crucibles to allow collection of any spalled corrosion products. The test environment was 13% CO_2 , 5% O_2 , 15% H_2O , 0.02% HCl with the balance nitrogen and a total gas flow of 150 ml·min⁻¹. This is an environment which has been established within the PREWIN European network on performance, reliability and emissions reductions in waste incinerators. Tests were run with a 160 hour hot dwell time and an 8 hour cold dwell time in which specimens were weighed and a 52.4 weight percent KCl + 47.6 weight percent K_2SO_4 deposit was applied by dipping. This corresponds to the eutectic with a melting point of 690°C. The target amount of deposit was 0.8 mg·cm⁻², which corresponds to 5 μg ·cm⁻²·h⁻¹. Testing was run for six cycles at either 550°C (1022°F) or 700°C (1292°F), giving a total hot dwell time of 960 hours.

After testing, specimens were wrapped in foil to retain as much as possible of the corrosion products then mounted in clear plastic and sectioned along the long axis. For post test metallography the long sides of the specimen were divided into eight sections of approximately equal size. Each section was examined at 320 x magnification in order to locate the area with smallest remaining metal thickness, m , where measurements were made. This area was then examined at 1620 x magnification so that a length of surface of 100 μm could be viewed in a single field and the thickness of remaining metal evaluated using a digital travelling stage. The metal loss was evaluated as

$$P = \frac{t-m}{2}$$

where t is thickness of the specimen measured for that position in the pre-test metrology and m is the remaining metal thickness.

This procedure meant that the entire cross section length was examined and each chosen field contained a local minimum in the remaining metal thickness which could be related to a reference point from the pre-test metrology. Manual selection of measurement points in this manner meant that the potential disadvantage with automatic measurements, i.e. that the most severe corrosion attack lay between measurement points, was avoided.

Results and discussion

Mass change and metrology

The net mass change curves at the two temperatures are shown in Figure 1. At the lower temperature of 550°C the carbon steel showed uneven mass change, which indicated that erratic spalling had occurred. The total amount of spall at the end of the test, Figure 2, was also highest for this material. At the higher temperature of 700°C the gross mass change of the carbon steel was higher by a factor of approximately 4, but the amount of spallation was less than at 550°C. The 2Cr steel (K21590) showed mass changes in parity with those of carbon steel, but less spallation at 550°C. The most unusual behaviour was shown by the 9Cr steel (K91560) which had similar levels of mass gains at the two test temperatures. The stainless steels S30403 and S30815 showed good reproducibility between duplicate specimens. At 550°C they showed low net and gross mass gains, with little spallation. The mass gains were not much higher than the total amount of deposited salt, which was a total of 4.8 mg·cm⁻² over the duration of the test. At 700°C the stainless steel gross mass gains were in the range 20–80 mg·cm⁻², with the lowest values being measured for S30815. The amount of spalled oxide was actually higher for the stainless steels than for the low alloyed steels; the consequence of this was that there was a net mass loss seen for all the stainless steels.

The mass changes may, however, give a misleading picture since they are unable to take two important factors into consideration. One is the occurrence of volatilisation, which causes a mass loss but is not possible to measure when performing testing on multiple specimens. Volatilisation may involve evaporation of the salt deposit or the formation of new volatile species such as metal chlorides or oxyhydroxides [10]. The other factor is the morphology of attack. Formation of a fine network of internal oxides or other corrosion products can render a component structurally unsound even though the total mass

Fig. 1 Net mass change curves at 550°C and 700°C in simulated biomass combustion environment with a KCl-K₂SO₄ deposit which was renewed every 160 hour cycle.

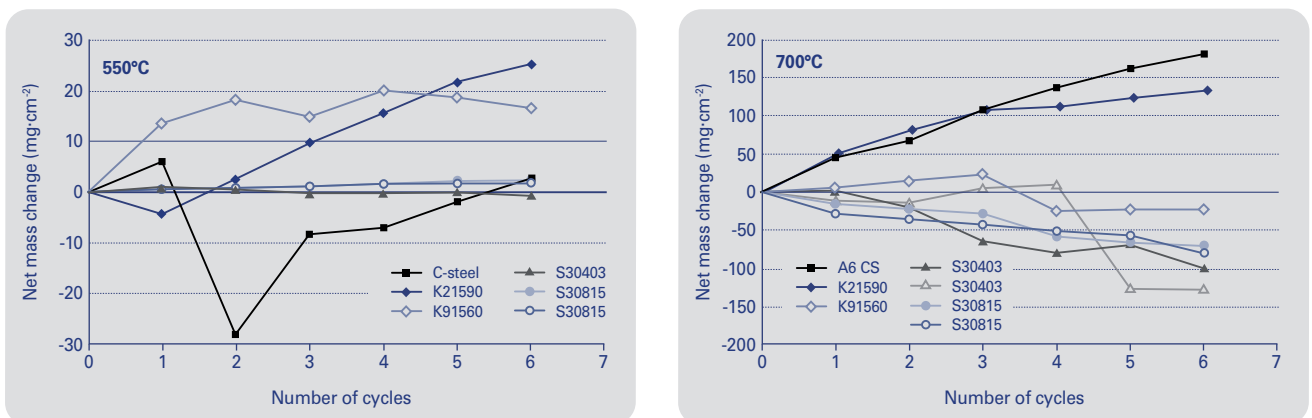


Fig. 2 Total net and gross mass changes and total amount of spall at the conclusion of testing in simulated biomass combustion environment with a total exposure time of 960 hours.

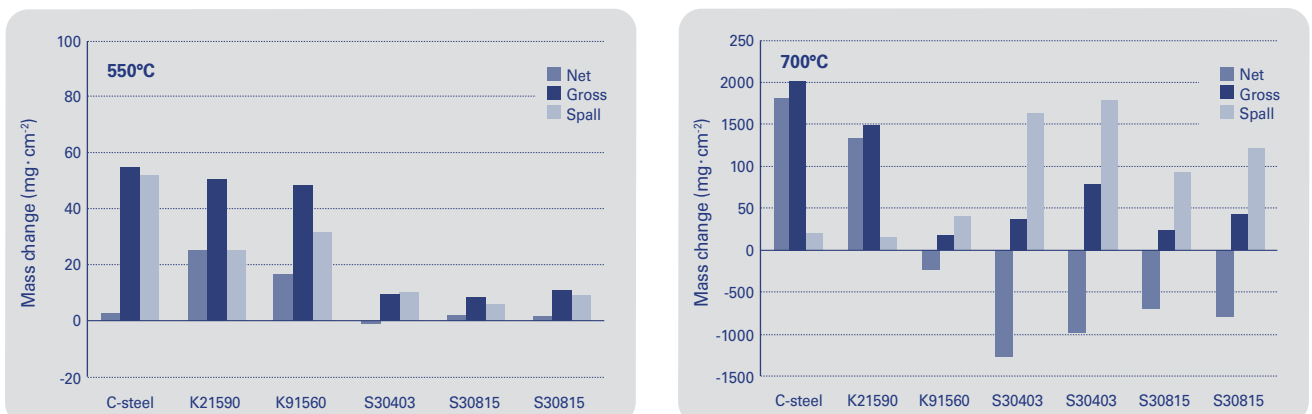
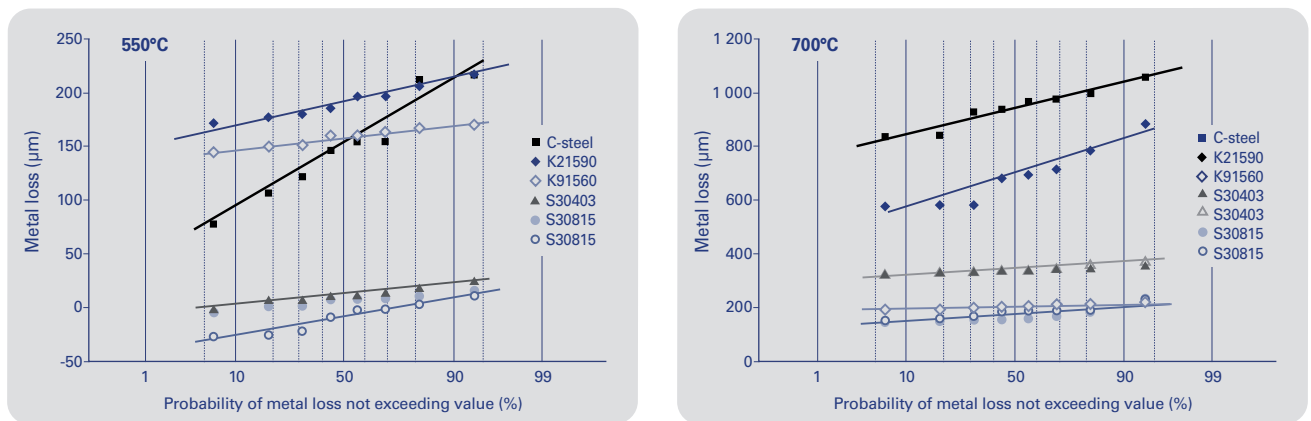
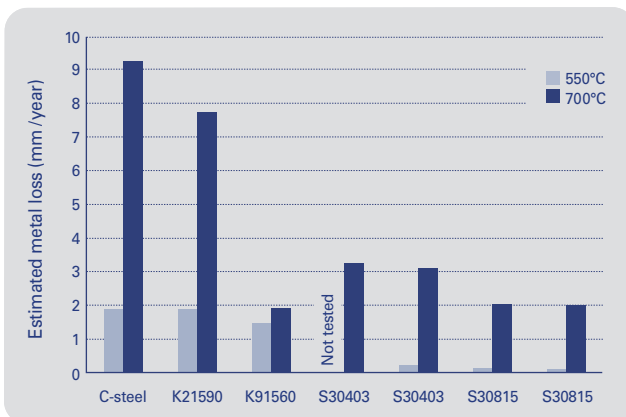
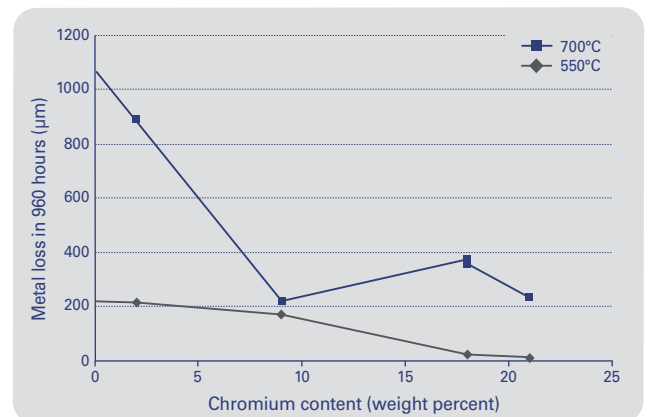


Fig. 3 Probability plots of metal loss obtained from post-test metallography**Fig. 4** Estimated annual metal loss based on an assumption of linear kinetics.**Fig. 5** Maximum metal loss after testing for 960 hours in the simulated biomass combustion environment, as a function of alloy chromium content. The anomalous behaviour of the 9% Cr steel at 700°C may be due to the variable incubation time reported for this material.

change is small. For this reason the use of metrology to assess the actual material damage is a vital part of materials evaluation in corrosion studies.

The results of measurements on cross sections are shown in Figure 3 and Figure 4. The metal loss followed a normal distribution, with higher standard deviations (reflected in the slope of the probability curves) for the lower alloyed materials. At 550°C the alloys fell very clearly into two groups. The carbon steel and low alloyed steels K21590 and K91560 showed high metal losses of over 150 µm, which extrapolates to around 2 mm·year⁻¹ if linear kinetics are assumed. The two stainless steels S30403 and S30815 exhibited very low losses. In some cases even negative values were recorded. This is because slight inaccuracies are inevitable when comparing pre-test micrometer measurements with post-test measurements in a travelling stage microscope, particularly when metal loss is so low.

At 700°C the extrapolated annual metal loss was 8–9 mm for the two lowest alloyed steels, i.e. approximately a factor 4 higher than at 550°C. Corresponding values for the stainless steels were 3 mm·year⁻¹ for S30403 and 2 mm·year⁻¹ for S30815. Both of the stainless steel grades showed excellent agreement between duplicate specimens. The only anomaly in the pattern was for the 9Cr steel K91560. This showed metal loss at 700°C which was only slightly higher than that at 550°C, Figure 5. This correlates to the observations from the mass change measurements, but is rather difficult to explain. One possibility is that it

may be related to the very large spread in incubation times for high temperature corrosion attack which have been reported for this alloy [11], and which mean that there is a shift between low and high corrosion rates. Longer term testing and/or a number of replicate specimens are clearly needed before firm conclusions can be drawn about this material.

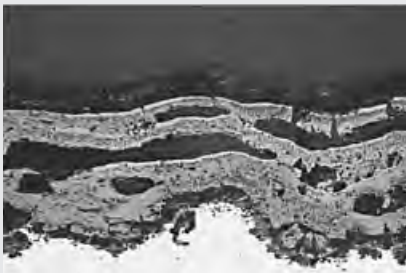
Corrosion attack and mechanisms

Figure 6 shows a comparison between light optical micrographs of the corrosion products on the specimens, all at the same magnification. The surface oxide was relatively uniform, with the exception of the undulating metal-oxide interface for carbon steel at 550°C.

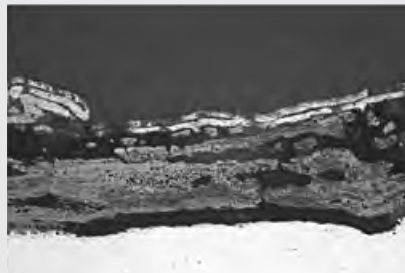
On the low alloy steels the corrosion products were primarily iron oxides, with very little presence of the environmental contaminants chlorine, potassium or sulphur, as illustrated

Fig. 6 Light optical micrographs of specimens after testing. The white outer layer is the protective foil used in specimen preparation and the same magnification has been used in all cases.

Carbon steel – 550°C



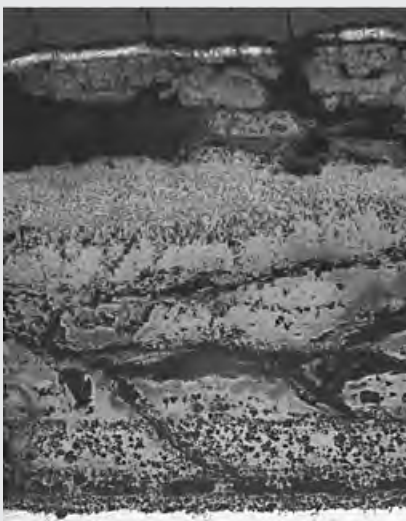
K21590 (2Cr) – 550°C



K91560 (9Cr) – 550°C



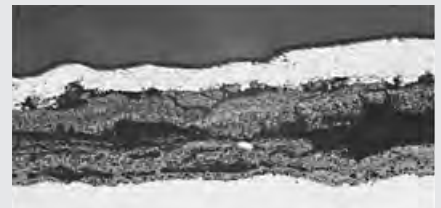
Carbon steel – 700°C



K21590 (2Cr) – 700°C



K91560 (9Cr) – 700°C



S30403 (18Cr) – 550°C



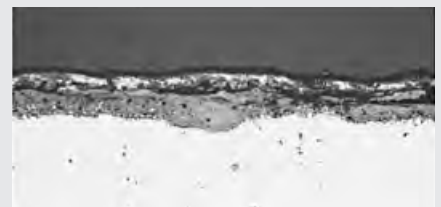
S30403 (18Cr) – 700°C



S30815 (21Cr) – 550°C



S30815 (21Cr) – 700°C



— 200 μm

Fig. 7 Backscattered electron image of corrosion products on carbon steel after testing at 700°C. All marked points are iron oxides with only traces of Cl (<0.1%) and K (<0.5%)

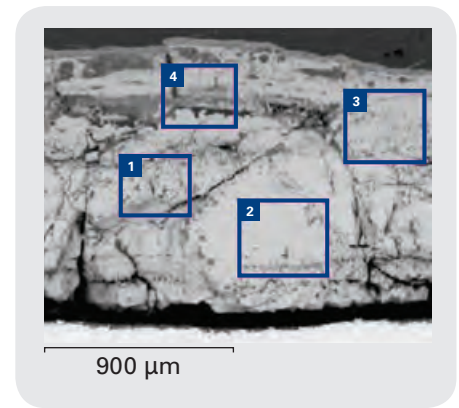
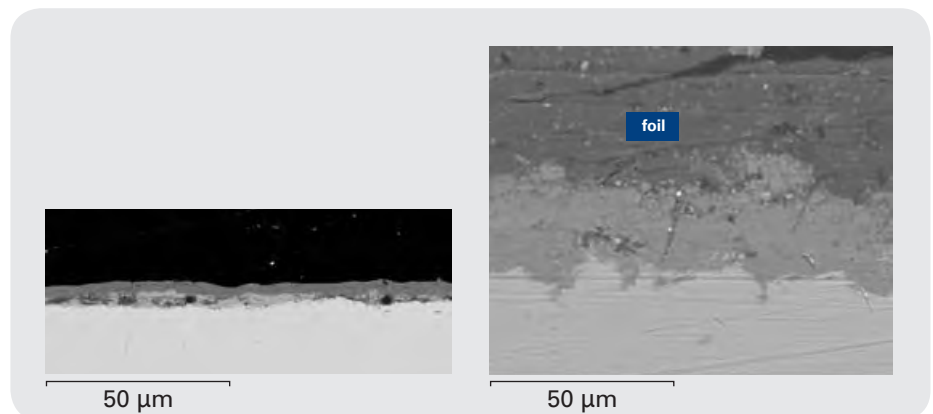


Fig. 8 S30403 after exposure in the low temperature biomass environment. The oxide layer is thin with no internal oxidation. The oxide consists mainly of iron (40–80 weight percent) and chromium (10–50%). Chloride was detected at low levels (0–2%) throughout the oxide and there were weak potassium signals (0–1%) but no significant amount of sulphur.



for the carbon steel at 700°C in Figure 7. This is in notable contrast to the behaviour in a simulated waste combustion environment previously reported [12], where a continuous layer of iron chlorides was seen at the carbon steel-oxide interface.

The stainless steels at 550°C showed a similar predominance of oxidation, with very little trace of K, S or Cl. Figure 8 shows that a single layer oxide around ~30 μm in thickness and containing 40–80% Fe and 10–50% Cr formed on S30403 (all analysis values are given in weight percent unless stated otherwise). Up to 2% Cl and 1% K could be detected within the oxide, but not as a clear separate phase, and there was no significant amount of sulphur. At the higher temperature of 700°C it may be recalled from the previous section that the majority of the oxide had spalled from the stainless steels. However, the micrographs in Figure 9 are taken at one of the places where the oxide scale was still attached to S30403, and show that in this case there was a thick, multi-layered oxide scale. The outer component was an iron-rich oxide containing up to 80% Fe, while the inner Cr-rich layer contained up to 75% Cr. There were low levels of potassium, <1% present in the Cr-oxide layer. Beneath the oxide scale there was a region of internal oxidation, where small oxide islands were surrounded by unoxidised metal. In this region it was possible to find small areas with high chloride contents, typically around 15% Cl, which provide strong indication that the chlorination mechanism described in the introduction is operative. The total thickness of the outer scale + inner oxidised region was ~300 μm. For comparison, the oxide formed on the same grade when exposed to synthetic air for 1000 hours at 700°C averaged only 6 μm [13]. The accelerating effect of the environmental contaminants applied in this work is thus very substantial.

S30815, which showed lower metal loss than S30403 at 700°C and a region where the oxide was still attached to the surface is shown in Figure 10. This gave a similar

Fig. 9 S30403 after exposure in the high temperature biomass environment. There is a thick outer oxide of 100–200µm comprising an outer layer of iron oxide and an inner chromium-rich oxide. Chlorides were present in the internally oxidised region and particles such as those arrowed in the enlarged area had typical compositions of 20% O, 15% Cl, 5% Cr, 40% Fe and 10% Ni.

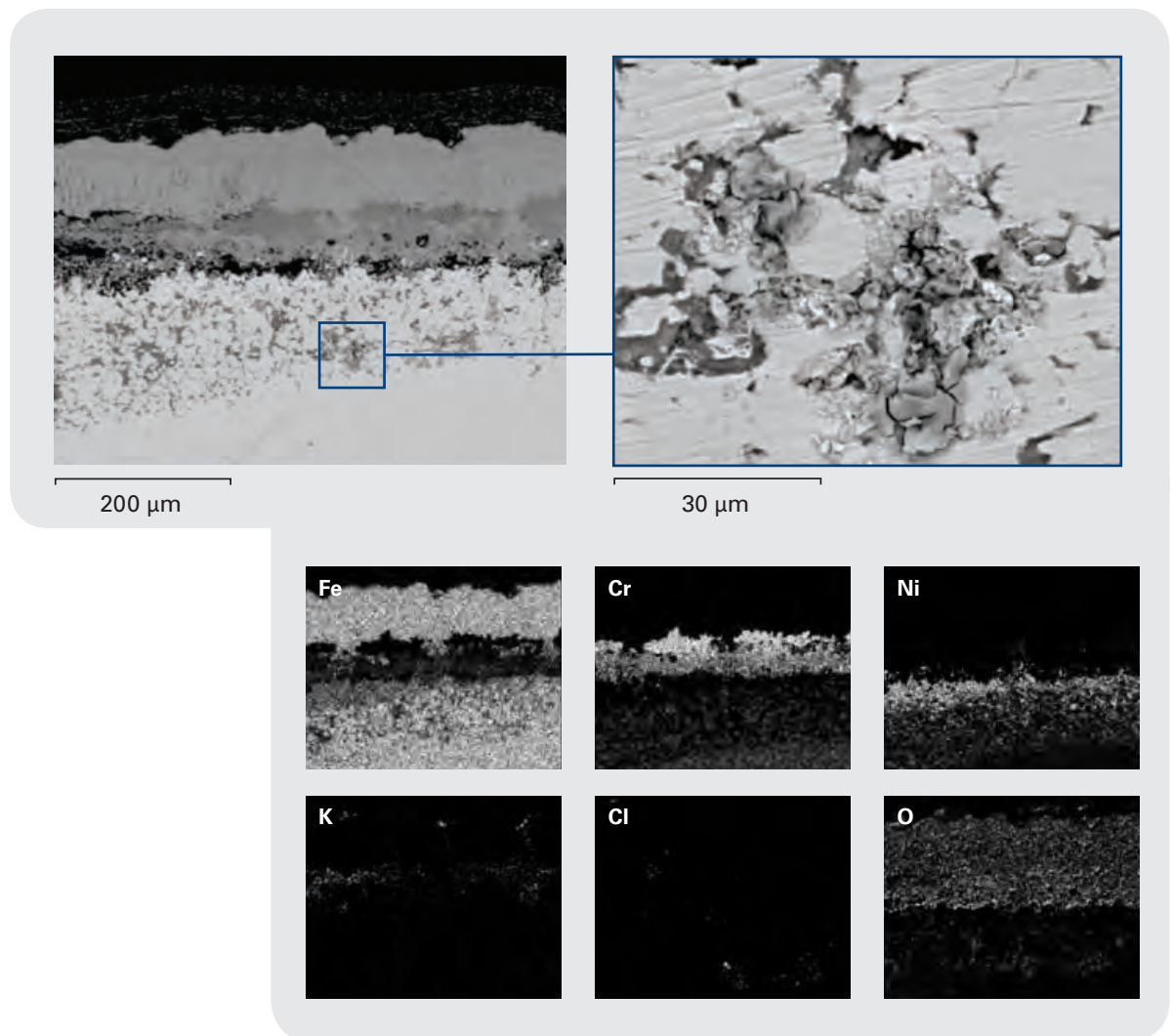
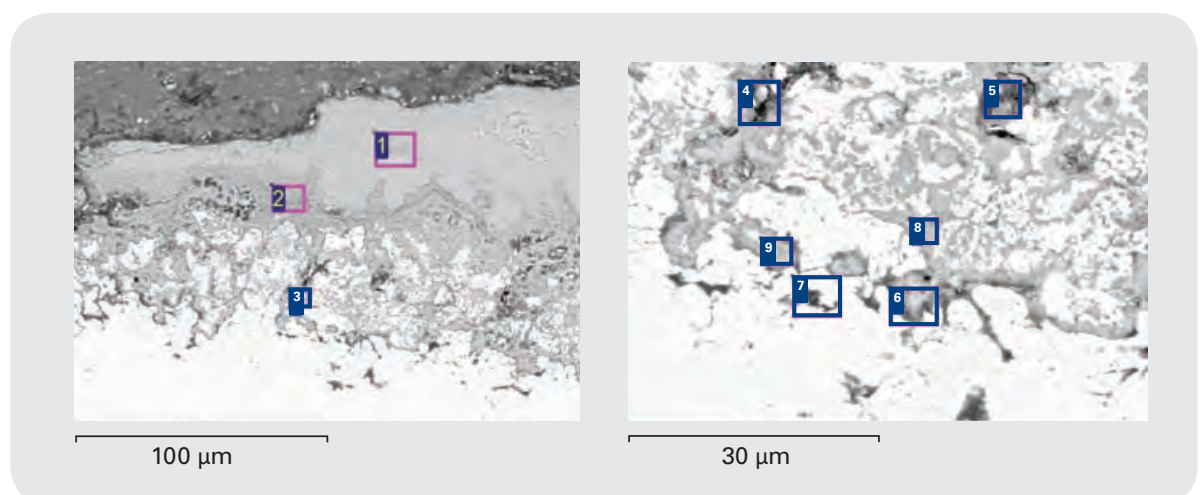


Fig. 10 S30815 after testing at 700°C. The outer oxide (1) contains ~60% Fe and 10% Cr while the inner oxide (2) comprises ~50% Cr and 20% Fe. All interface areas (4) to (9) are chromium-dominated oxide with up to 10% Si but less than 0.3% Cl and no measurable amounts of potassium.



picture in that there was an outer iron-rich oxide scale and an inner Cr-rich scale, also a region under the scale in which partial internal oxidation had occurred. However, the notable difference compared to S30403 was the lower amount of chlorine and the presence of silicon oxides within this internally oxidised region for S30815. The area analyses yielded up to 10% silicon, locally the amounts are therefore appreciably higher and it is reasonable to assume that a silicon oxide phase is present. This material is intentionally alloyed with ~1.5% silicon to improve the high temperature oxidation and corrosion resistance, and it seems that this has had a beneficial effect in the present case by blocking the sites at which chlorides would otherwise form.

Conclusions

High temperature corrosion of low alloy and stainless steels in a simulated biomass combustion environment with a periodically renewed deposit of $\text{KCl} + \text{K}_2\text{SO}_4$ resulted in an accelerated oxidation process. The corrosion product layer was relatively uniform, with only a small amount of internal oxidation/corrosion and a minor presence of Cl at the metal-oxide interface.

Evaluation of corrosion rates by metrology indicated that an appreciable reduction in materials wastage rates can be achieved by replacement of low alloyed steels by stainless steel. The high temperature stainless steel S30815 showed a corrosion rate which was five times lower than carbon steel at 700°C and twenty times lower at 550°C. The superior performance of S30815 over the standard S30403 grade is attributed to silicon alloying, which at least partially blocks sites at which metal chlorides can form.

Acknowledgements

This research project was carried out with a financial grant from the Research Fund for Coal and Steel of the European Community under contract no. RFS-CR-03020.

References

- [1] Y.Y. Lee and M.J. McNallan, Ignition of nickel in environments containing oxygen and chlorine, *Metallurg. Trans. Vol 18A*, p. 1099, (1987)
- [2] E. Reese and H.J. Grabke, Effects of chlorides on the oxidation of the 2.25Cr-1Mo Steel, *Materials and Corrosion* 43, pp.547–557 (1992)
- [3] H.J. Grabke, Fundamental mechanisms of attack of chlorine, HCl and chlorides on steels and high temperature alloys in the temperature range 400° to 900°C, *Incinerating municipal and Industrial Waste New York Hemisphere Publ. Corp.* pp. 161–176 43 (1991)
- [4] M. Spiegel, Reactions between gas phase, deposits and metallic materials in chlorine containing atmospheres, *Materials at High Temperatures*, 14, pp. 221–226, (1997)
- [5] J-M. Abels and H.-H. Strehblow, A surface analytical approach to the high temperature chlorination behaviour of Inconel 600 at 700°C, *Corr. Sci.*, Vol. 39, No. 1 pp. 115–132 43 (1997)
- [6] P. Szakálos, P. Henderson, R. Pettersson, Mechanisms of chlorine induced corrosion and effect of sulphur additions in superheater corrosion in biomass- and waste fired boilers, 16th International Corrosion Congress (ICC), September 19 to 24, Beijing, China (2005)
- [7] A. Karlsson, P. Møller, and V. Johansen, Iron and steel corrosion in a system of O₂, SO₂ and alkali chloride. The formation of low melting point salt mixtures, *Corrosion Science*, 30, pp. 153–158, (1990)
- [8] P. Kofstad, *High Temperature Corrosion*, Elsevier Applied Science, New York, 1988.
- [9] J. Pettersson, H. Asteman, J-E Svensson, L-G Johansson, KCl induced corrosion of a 304-type austenitic stainless steel at 600°C, *Oxidation of Metals* 64:1-2 pp. 23–41 (Aug 2005)
- [10] B.B.Ebbinghaus, Introduction to the possibilities of chromium evaporation according to the thermodynamics calculation, *Combustion and Flame* 93, pp. 119–137 (1993)
- [11] M Schutze et al., Cyclic oxidation testing – Development of a code of practice for the characterisation of high temperature materials performance (COTEST), G6RD-CT-2001-00639
- [12] R. Pettersson, J. Flyg, P. Viklund, Materials performance in simulated waste combustion environments, *Corrosion Engineering, Science and Technology* 43:2 pp. 123–128 (June 2008)
- [13] R. Pettersson, J. Flyg, K. Göransson, M. Willför, Evaluation of stainless steels for combustion environments, Report TO43-14 (2003) from Jernkontoret, the Swedish Steel Producers Association

Stainless steels in waste and biomass power plant applications

Rachel Pettersson, Outokumpu Stainless AB, Sweden

Arne Bergquist, Outokumpu Stainless AB, Sweden

Jesper Flyg, Swerea KIMAB AB, Sweden

Bernd Beckers, Outokumpu N.V., Belgium

Abstract

Power generation, particularly from corrosive fuels such as biomass and waste, places severe demands on construction materials in many parts of the boiler and flue gas cleaning systems. Stainless steels are attractive materials alternatives in many cases, and the correct selection of grades can make a significant contribution to the extension of equipment lifetimes.

Corrosion data and application examples are given in which high temperature steels are used in waterwalls and superheaters. Materials selection for boiler components is addressed, together with a discussion on the potential for increasing steam temperatures. Finally, the use of corrosion-resistant grades for flue gas cleaning is presented together with results from field testing.

Key words: corrosion, power generation, superheater, flue gas

1. Introduction

A thermal power plant presents a serious challenge to the materials engineer or corrosion scientist. Multiple corrosive species are present and the conditions also involve complicating factors such as high flow rates, erosion, deposition and condensation. The present work focuses on power generation from renewable sources, which means biomass, waste, or frequently a combination of the two. Such renewable fuel sources are a critically important component of sustainable energy production. The use of waste materials as fuel also has the environmental advantages of reducing landfill and in this way can be regarded as having double “green” credentials.

In coal or oil fired power plants, creep is often an issue because of the high temperatures involved. In contrast, the primary issue in waste and biomass combustion is that of corrosion, which makes it necessary to limit the steam temperatures. The primary species of concern are alkali metals from biomass and chlorine species in waste combustion. The presence of heavy metals is particularly damaging, because of their propensity to form low melting point eutectic salts, which can drastically increase the rate of corrosion [1, 2].

The areas of a power plant of concern in corrosion terms include both the boiler, where the main issue is high temperature corrosion, and the lower temperature areas in the flue gas cleaning system, where aqueous corrosion issues dominate. In the boiler, the bed or grate area, where the solid state combustion occurs, is characterised by erosion from moving fuel and/or from sand in a fluidised bed; large temperature gradients and fluctuations, also locally reducing conditions arising from substoichiometry or stratification in the boiler. The second critical area is the tubing system and support system, particularly the superheaters in which steam is given the final boost in temperature before being sent to the steam turbine. Here the main issue is one of corrosion under ash and salt deposits. Seamless tubes are often employed, but welded tubes can be attractive alternatives for many dimensions. The metal temperatures of cooled components are typically in the

region of 300–400°C for waste combustion plants and 450–550°C for biomass, but appreciably higher temperatures are encountered by uncooled components such as tube shields and fixtures. As the flue gas is successively cooled, the main issue becomes one of condensation. Very aggressive acidic condensates form when the dewpoint for hydrochloric acid and/or sulphuric acid are reached, giving a severe aqueous corrosion problem.

Another aspect which makes thermal power plants particularly interesting from a materials point of view is the enormous range of ways in which corrosion issues may be tackled. In many applications, materials selection is limited to, say, the choice of an austenitic or duplex stainless steel. In renewable fuel power plants metallic materials choices range from carbon steel through stainless steels to nickel-base alloys, and the materials solutions may also include ceramics, such as the spray coatings on waterwalls, and polymers, particularly the use of GRP in flue gas cleaning. In this work corrosion issues in the two areas outlined above are examined and results are presented from both laboratory testing in simulated environments and field testing of probes and test coupons. The former approach has the advantage of allowing strict control of the environment, so that critical parameters may be identified, while the latter shows the real situation, albeit with questions regarding whether placement of test coupons is representative and reproducible. The true strength is when the two approaches can be combined and give a coherent whole.

2. Experimental

2.1 Simulated boiler environments

The materials used for the laboratory tests in simulated superheater environments are given in Table 1. The stainless steels 253 MA[®] and 310S were from Outokumpu stock, while the nickel-base specimens were produced by Inasmet, San Sebastián, Spain. Two MIG weld overlay passes were made on carbon steel using Inconel 625 electrodes with a composition of Ni-22Cr-9Mo-3Nb or Hastelloy C-276 with a composition of 16Cr-16Mo-4W-6Fe.

Materials employed for simulated superheater corrosion tests. All values are given in weight percent.

Table 1

Grade	EN	UNS	Fe	Cr	Ni	Mo	Si	Mn	Other
T22	1.7380	K21590		2.3		0.9	0.2	0.5	
253 MA [®]	1.4835	S30815	Bal	21.0	10.9	0.2	1.6	0.6	Ce
310S	1.4845	S31008	Bal	25.1	19.4	0.2	0.6	1.0	
625 weld*			3.0	21.3	62.6	8.9			3Nb
C-276 weld*			11.0	14.9	54.9	15.5			3.5W

*Compositions analysed 6 mm from fusion line

Test specimens of approximate dimensions 16 x 12 x 3 mm were wet surface ground to 600 grit SiC, weighed and measured before testing and placed in individual crucibles to allow collection of any spalled corrosion products. The test environments were as specified in Table 2 and have been established within the PREWIN European network on Performance, Reliability and Emissions reductions in Waste Incinerators and used in a number of published works [2, 3]. Tests were run with a 160 hour hot dwell time and an 8 hour cold dwell time in which specimens were weighed and the deposit applied by dipping to a target amount of dry salt of 0.8 mg·cm⁻², which corresponds to 5 µg·cm⁻²·h⁻¹. The biomass deposit of 52.4 weight percent KCl + 47.6 weight percent K₂SO₄ corresponds to the eutectic with a melting point of 690°C while the waste deposit has a specified eutectic temperature of 230°C [4]. The gas flow rate during testing was 150 ml·min⁻¹, which corresponded to a flow rate past the specimens of 4.3 mm·s⁻¹.

After testing, specimens were wrapped in foil to retain as much as possible of the

Conditions employed for laboratory simulation of deposit conditions in boilers.

Table 2

	T (°C)	Bal	O ₂ (%)	H ₂ O (%)	SO ₂ (%)	HCl (%)	Other	Deposits	Cycles
Waste Low T	320	N ₂	8	15	0.02	0.2		50% ¹ KCl 50% ¹ ZnCl ₂	14
Waste High T	420	N ₂	8	15	0.02	0.2		50% ¹ KCl 50% ¹ ZnCl ₂	12
Biomass – Low T	550	N ₂	5	15	–	0.02	13% CO ₂	52.4% ² KCl 47.6% ² K ₂ SO ₄	6
Biomass – High T	700	N ₂	5	15	–	0.02	13% CO ₂	52.4% ² KCl 47.6% ² K ₂ SO ₄	6

¹molar percent ²percent by weight

corrosion products then mounted in clear plastic and sectioned along the long axis. For post test metallography the long sides of the specimen were divided into eight sections of approximately equal size. Each section was examined at 320 x magnification in order to locate the area with smallest remaining metal thickness, *m*, where measurements were made. This area was then examined at 1620 x magnification so that a length of surface of 100 µm could be viewed in a single field and the thickness of remaining metal evaluated using a digital travelling stage. The metal loss was evaluated as

$$P = \frac{t-m}{2}$$

where *t* is thickness of the specimen measured for that position in the pre-test metrology and *m* is the remaining metal thickness.

2.2 Condensate testing

A combination of field testing and laboratory testing was used to evaluate the corrosion performance of different materials in flue gas cleaning systems. The materials investigated are given Table 3. 254 SMO[®] and 654 SMO[®] were obtained from Outokumpu stock, 317 LMN, 2205 and C-276 were provided by Industeel, now part of Arcelor Mittal, within the framework of a European research project [5], as was 1.4410 (Sandvik SAF 2507) from Sandvik Steel.

Materials employed for simulated superheater corrosion tests. All values are given in weight percent.

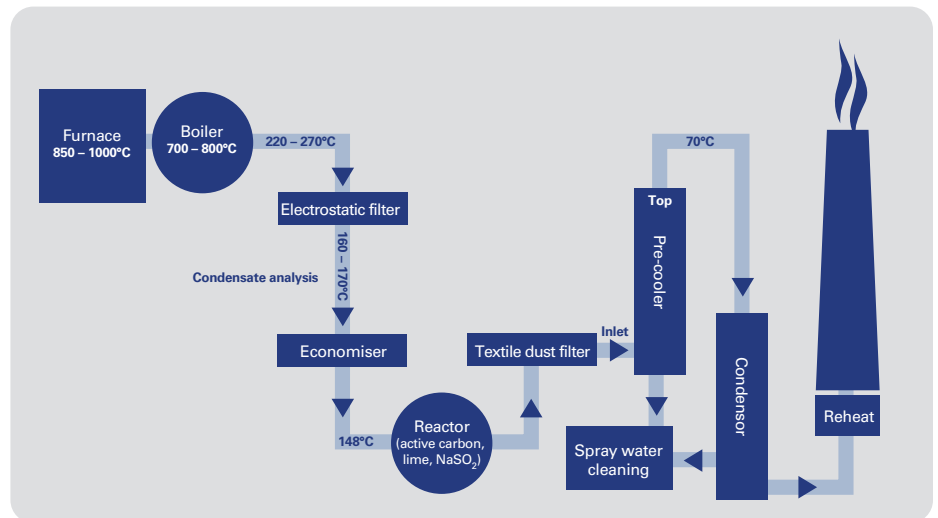
Table 3

Grade	EN	UNS	Cr	Ni	Mo	N	W	PRE*
317 LMN	1.4439	S31726	17.2	12.9	4.1	0.14	0.04	32.9
254 SMO [®]	1.4547	S31254	19.8	17.9	6.0	0.20	0	43.0
654 SMO [®]	1.4652	S32654	24.3	21.8	7.3	0.52	0	56.6
2205	1.4462	S31803	22.3	5.2	3.2	0.17	0	35.6
2507	1.4410	S32750	25.3	7.1	3.9	0.26	0	42.4
C-276	2.4819	N10276	16	57.6	16.2	0	3.3	74.9

*Pitting resistance equivalent, PRE = %Cr + 3.3 (%Mo + ½%W) + 16 (%N)

A waste-fired district heating plant, with two boilers of 6MW + 25 MW connected to a common gas cleaning system, was used for field testing, Figure 1. Test coupons of dimensions 60 x 60 mm, with a weld and MTI multi-crevice washer, were mounted on a base plate in C-276 and placed at two locations in the pre-cooler. Condensate was removed between the electrostatic filter and the economiser using a cooled probe [5] and analysed using Inductively Coupled Plasma Time of Flight Mass Spectrometry (ICP-TOFMS) for cations and ion chromatography for anions.

Fig. 1 Schematic illustration of the waste-fired district heating boiler used for condensate analysis and field testing at the inlet and top of the pre-cooler.



Based on these analyses, a number of synthetic condensate solutions were prepared according to Table 4 and used for laboratory tests. Specimens were in the form of coupons 25 x 25 mm which were wet surface ground to 600 mesh SiC paper less than an hour before electrochemical testing. Specimens were mounted in a flushed-port cell to avoid crevice effects and solutions were aerated, since this was considered more representative of the application, in which there is normally an oxygen excess present. The corrosion potential was first measured for 5 minutes then the potential scanned in the anodic direction at 20 mV·min⁻¹ starting at a potential 100 mV below the corrosion potential.

Environments used for laboratory evaluation of corrosion in synthetic condensates.

Table 4

Environment	HCl conc.	Temp.	Other
1	1.6M	70°C	
2	0.8M	70°C	
3	1.6M	50°C	
4	0.8M	50°C	
5	0.2M	50°C	
HCl + H ₂ SO ₄ (sulphate addition)	0.8M	70°C	0.2M H ₂ SO ₄
HCl/H ₂ SO ₄ (sulphate replacement)	0.4M	70°C	0.2M H ₂ SO ₄
HCl/HNO ₃	0.79M	70°C	0.01M HNO ₃
HCl/HBr	0.79M	70°C	0.01M HBr
HCl/HF	0.79M	70°C	0.01M HF
Complex	0.79M	70°C	0.01M HNO ₃ + 0.01M HBr + 0.01M HF
Metal	0.79M	70°C	0.025M AlCl ₃ + 0.025M FeCl ₃ + 0.025M NaCl + 0.025M ZnCl ₂

4. Results and discussion

4.1 Testing in simulated boiler environments

Maximum metal losses from the metallographic analysis of specimens exposed in the simulated biomass superheater environment are shown in Figure 2. Also shown is the corresponding total gross mass change i.e. including the mass of spalled oxide and corrosion products. In both cases the assumption has been made that the corrosion process is linear, so that data from a total hot dwell time of 960 hours at the test temperature can be extrapolated to an annual metal loss or mass change. This assumption is reasonable since a large amount of spallation is occurring. Agreement between the two types of data is good, although the metal loss data has the advantage that it shows the true loss of functional metal section, while the mass change data is affected by multiple processes such as oxide formation, spallation and evaporation.

At the lower test temperature of 550°C metal loss was highest for T22, almost 2 mm·year⁻¹, while the two stainless steels 253 MA[®] and 310S showed metal losses of ~0.1 mm·year⁻¹ or less and actually performed better than the overlay nickel-base weld metals. The implications in terms of component lifetime of upgrading superheater materials from a 2Cr-1Mo steel to an austenitic stainless steel are thus very substantial.

Fig. 2 Maximum metal loss in simulated biomass environments and measured gross mass change.

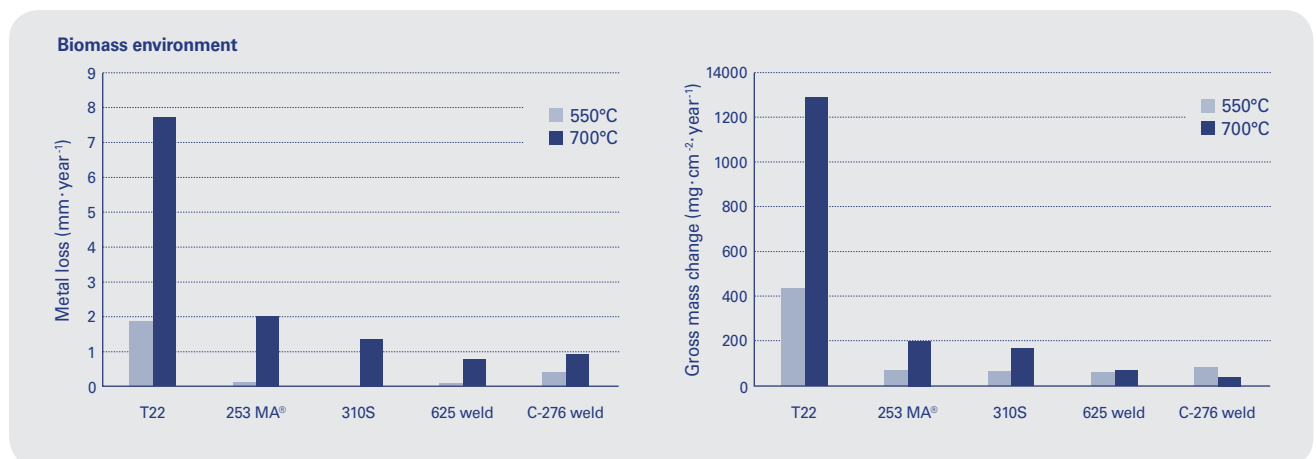
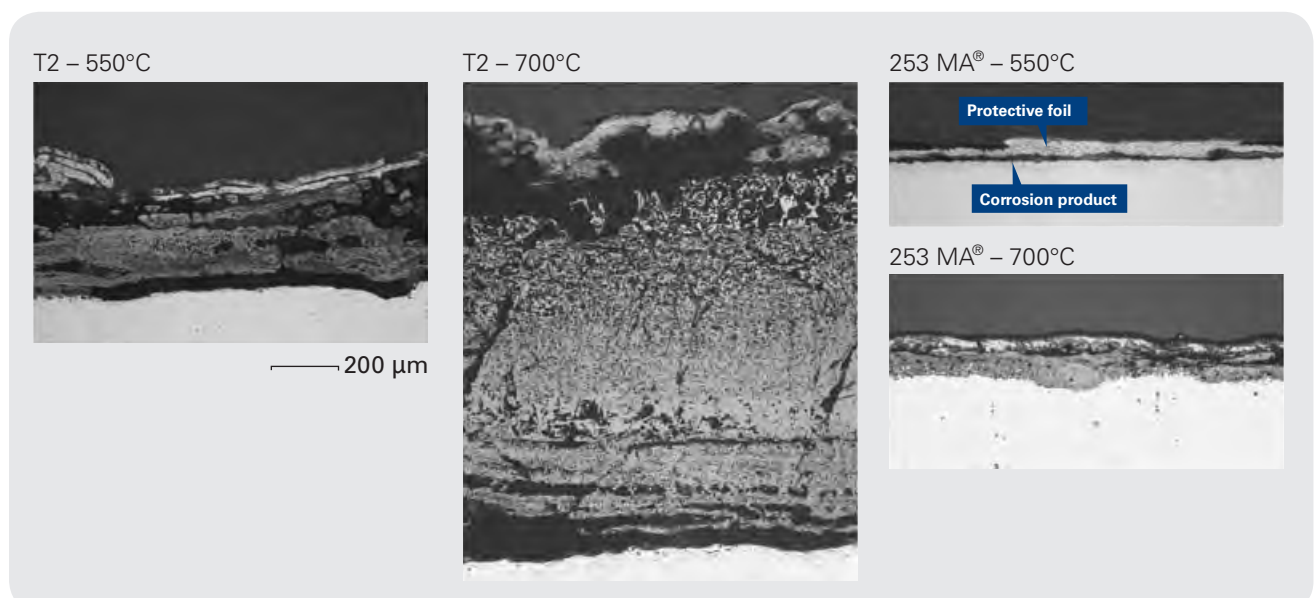


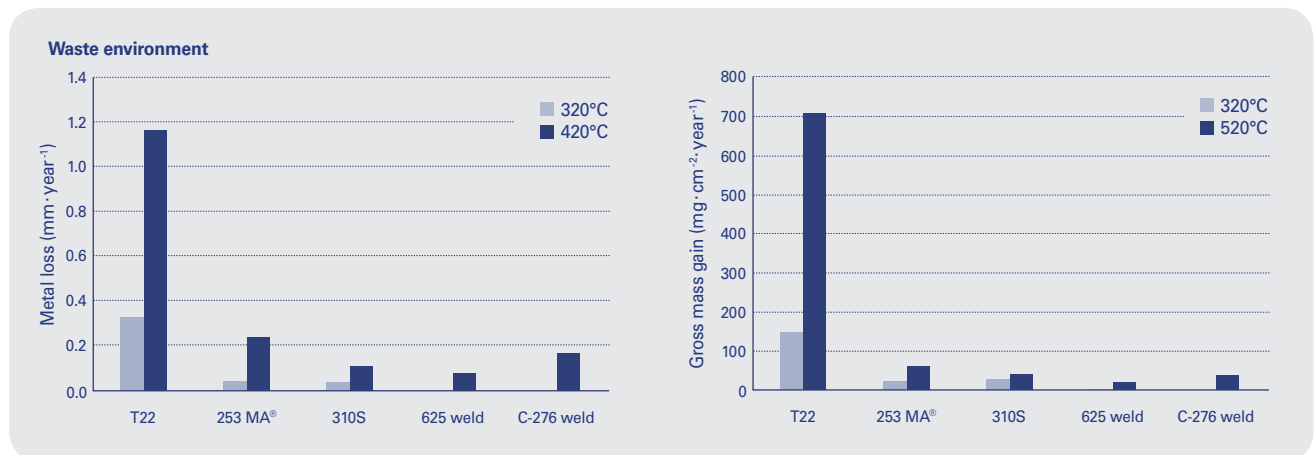
Fig. 3 Light optical micrographs showing corrosion products on T22 and 253 MA after testing in the simulated biomass combustion environments for a total hot dwell time of 960 hours.



The nickel-base alloys do not seem to show a performance which could merit the appreciably higher alloy cost involved. Increasing the temperature to 700°C, which is much higher than the current operating range for biomass boilers, naturally increased the corrosion rates for all materials. The corrosion rate of over 7 mm·year⁻¹ renders T22 highly unsuitable, while the corrosion rates were 1–2 mm·year⁻¹ for the stainless steels and ~1 mm·year⁻¹ for the nickel-base alloys. Examples of the corrosion attack are seen in the micrographs in Figure 3.

Corresponding metal loss and mass change data for the simulated waste combustion environments are shown in Figure 4. The first point to note is that the metal losses are appreciably lower than in the simulated biomass environments, by around an order of magnitude. The mitigating effect of the lower temperatures clearly outweighs the detrimental effect of the more damaging chloride salt deposit. Ranking of the materials shows similar trends to the biomass environment, with the highest metal losses unsurprisingly been shown by the low alloyed T22. At the lower temperature of 320°C the nickel-base alloys show barely measurable metal loss, but even that for the two stainless steels 253 MA[®] and 310S it is less than 50 µm·year⁻¹. Raising the temperature to 420°C increases metal loss for both austenitic stainless steels and nickel base alloys to ~100–200 µm·year⁻¹, so the utilisation of the former becomes comparatively advantageous.

Fig. 4 Maximum metal loss in simulated waste superheater environments and measured gross mass change.



The metal loss data indicates that if the low-alloyed T22 is replaced by 253 MA[®] or 310S stainless steel, the temperature in a waste-fired boiler could be increased from 320°C to 420°C and the corrosion rate nevertheless decreased. Caution must naturally be exercised in applying this data to the more complex situation in a waste combustion plant, but the results do indicate the potential gains from the use of more advanced materials.

There is a continual drive towards higher steam temperatures in order to improve the electricity production efficiency in WTE (waste-to-energy) plants. The total efficiency is difficult to predict, since it depends on such factors as the number of reheat steps, pumping systems etc. However, a rough estimate of the potential energy gains attainable may be obtained from the theoretical maximum efficiency in a Carnot cycle, which is given by

$$\eta = 1 - \left(\frac{T_{\min}}{T_{\max}} \right)$$

For $T_{\min}=303\text{K}$ (30°C) an increase in T_{\max} from 593K (320°C) to 693K (420°C) could potentially give a maximum of 15% increase in energy efficiency based on the laboratory data.

4.2 Comparison with field testing data

In order to put these results into perspective, some data from field exposures in a combined heat (69MW) and power (35MW) bubbling fluidised bed boiler fired with wood chips, demolition waste and coal, are presented in Figure 5 [6, 7], and were obtained after 10 weeks of testing probes with a metal temperature of 600°C. Once again, the data have been extrapolated, using an assumption of linearity, to give an annual metal wastage

figure. Two interesting features are seen here, the first is that the corrosion rates are in reasonable agreement with the laboratory testing. The T22 (2Cr-1Mo) showed a corrosion rate of $\sim 3 \text{ mm}\cdot\text{year}^{-1}$ which falls into the span of $\sim 2 \text{ mm}\cdot\text{year}^{-1}$ at 550°C and $\sim 8 \text{ mm}\cdot\text{year}^{-1}$ at 700°C in the simulated laboratory environment. The situation for stainless steel actually appears slightly better in the field tests, with metal losses of $\sim 0.1 \text{ mm}\cdot\text{year}^{-1}$, to be compared with $<0.1 \text{ mm}\cdot\text{year}^{-1}$ at 550°C or $1.3 \text{ mm}\cdot\text{year}^{-1}$ at 700°C in laboratory tests.

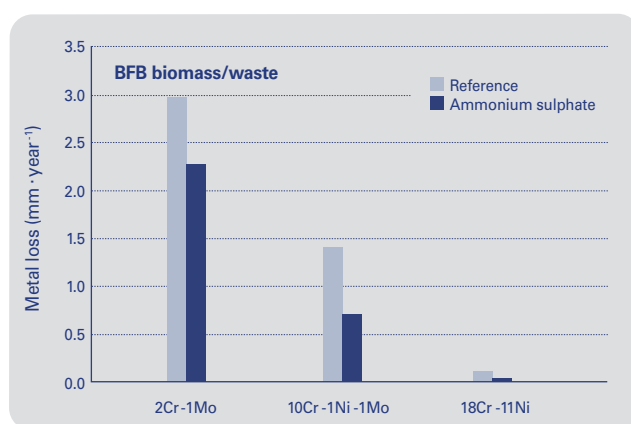
A second interesting feature seen in the data in Figure 5 is that additions of sulphur, in this case in the form of ammonium sulphate solution, clearly decrease the corrosion rate. Sulphur additions are used in a number of commercial boilers, often using the ammonium sulphate “ChlorOut” technology developed by Vattenfall [7] in order to mitigate chloride-induced corrosion under deposits. The sulphur, or sulphate, promotes the sulphidation of alkali chlorides in the flue gas so that less of the latter condense and the deposit thus becomes less corrosive. In the case shown in Figure 5 the sulphate additions give $\sim 20\%$ reduction in the metal wastage rate for T22, while for the higher alloyed stainless steels the figure is $>50\%$. The question of the impact on the corrosion of nickel-base alloys, which are recognised to be particularly sensitive to sulphidation attack, is one focus in ongoing work.

A similar beneficial result of both alloying level and ammonium sulphate additions has been reported [8]. In this case T22 and 304 were exposed in a waste-fired CFB boiler burning a mixture of household and industrial waste. The exposures were for 4 hours with a metal temperature of 500°C . In this case T22 showed severe oxidation, with the formation of underlying chlorides, which were considerably decreased when ammonium sulphate was added. The type 304 stainless steel also showed some ingress of chlorine, but this was much less pronounced than for T22, indicating that the chromia scale played a protective role. In this case too there was a measurable reduction in the amount of corrosion damage when ammonium sulphate was added to the boiler.

A further comparison against which the laboratory data in §4.1 can be compared, is provided by waterwall testing [9], actually in the same CFB boiler as described above. Overlay weld panels were exposed for a total of 7727 hours, after which disc specimens were removed for examination. The results in Table 5 show that the iron-containing nickel-

base overlay 650 showed the worst performance, with extensive pitting up to 1 mm in depth. This was not picked up in the in-situ thickness measurements which seem at best to give an average metal loss which includes the pits. The stainless steel 310 gave a higher metal loss of 1.13 mm, which converts to $1.3 \text{ mm}\cdot\text{year}^{-1}$. The temperature is difficult to determine at the waterwalls and fluctuates a great deal. It can nevertheless be concluded that the metal loss is in the same region as that in the laboratory test data in Figure 2. Interestingly, the stainless steel shows no pitting, only uniform metal wastage. The amount of metal loss is on a par with that of the nickel-base alloy 650, but the difference is that the even wastage for the stainless steel can easily be identified and monitored using in-situ thickness measuring devices. Even the most resistant material in the comparison, the nickel-base alloy 625, showed pitting, albeit less than for alloy 650.

Fig. 5 Field testing data from cooled superheater probes in a BFB boiler fired with biomass and waste [6, 7].



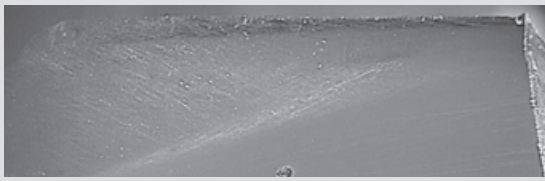
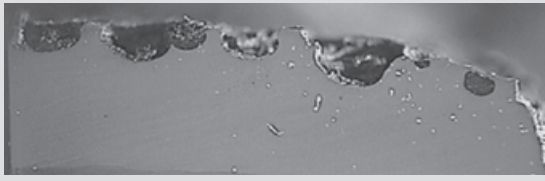
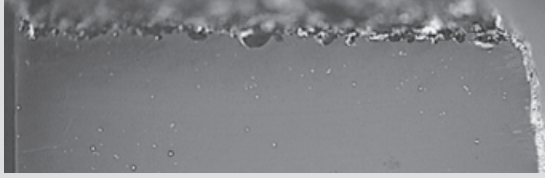
4.3 Condensate analysis and testing in condensate

Dewpoint measurements in the waste district heating plant yielded a dewpoint of 67°C at the measurement position between the electrostatic filter and economiser. Analysis of removed condensate at two different temperatures is given in Table 6 and shows the principal component to be hydrochloric acid, with some metal ions and sulphate present. It had been suspected that appreciable levels of fluoride, bromide or nitrate would be detected, but all of these were at such low levels as to be below the analysis limit.

In the first series of laboratory tests a simple hydrochloric acid environment was used,

Results from 7727 hour field testing of overlay welded waterwall panels

Table 5

Designation and filler composition	Disc cross section (width ~10mm)	Average in-situ metal loss (mm)	Max pit depth (mm)
310 (Fe-26Cr-21Ni)		1.13	≤ 0.05
Alloy 650 (Ni-20Cr-12Mo-14Fe-1.5W)		0.68	0.96
Alloy 625 (Ni-22Cr-9Mo-3.6Nb)		0.27	0.29

Analysis (in mmol) of four samples of condensate removed from gas cleaning system of the waste-fired district heating boiler.

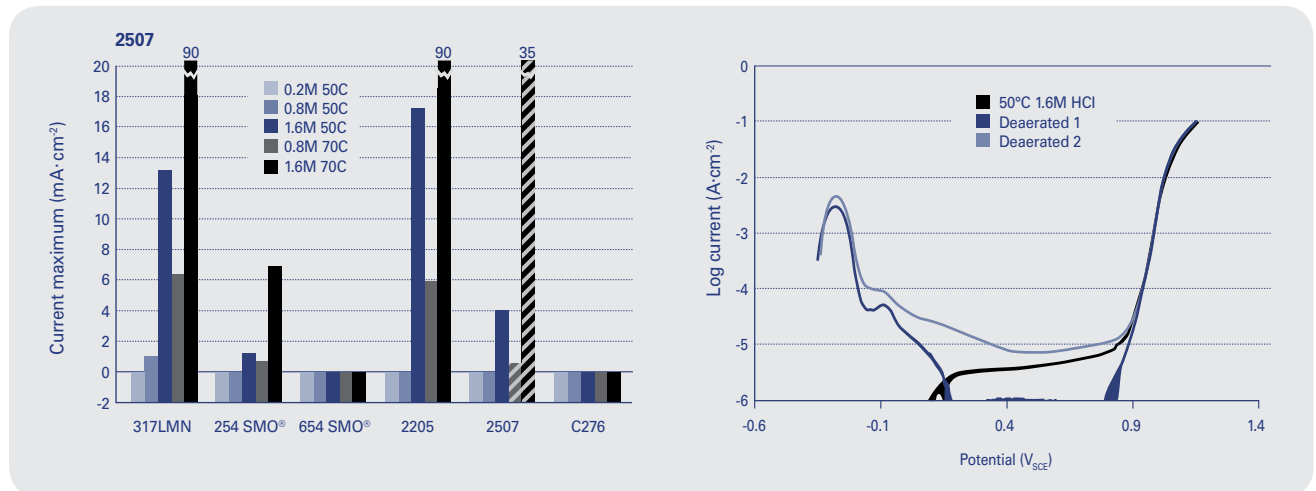
Table 6

	35°C			55°C
H ⁺	25	29	45	832
Al	0	0	2	51
Na	2	3	18	139
Zn	0	0	0	5
Fe	0	0	0	3
Pb	0	0	0	1
Cl ⁻	23	28	59	1016
SO ₄ ²⁻	1	0	2	20

and polarisation curves employed to give a rapid overview of the corrosion behaviour. The results in Figure 6 show that in the mildest environment, 0.2M HCl at 50°C, all steels were passive, with no active peak. Increasing the concentration to 0.8M caused 317 LMN to shift to active corrosion, and a further step up to 1.6M caused 254 SMO[®] and both the duplex stainless steels to activate. Particularly 2205 showed a high peak current density. Only the superaustenitic stainless steel 654 SMO[®] and the nickel-base alloy C-276 remained passive.

Increasing the test temperature to 70°C gave a the same type of behaviour, with similar levels of active corrosion for 317 LMN and 2205. Once again the superaustenitic 654 SMO[®] and the nickel-base C-276 remained passive. The 6% Mo superaustenitic 254 SMO[®] showed a moderate degree of corrosion, but rather surprisingly the superduplex 2507 remained passive. This was in contrast to the behaviour at 50°C, where its performance was inferior to 254 SMO[®]. However, two points indicate that this passivity of 2507 was not entirely stable. Firstly the corrosion potential during the tests was positive, indicating that it was the aeration level which was suppressing activation. Secondly, a series of tests on the same materials but using deaeration and activation at a low potential at the start of the test provoked depassivation of 2507. This gave maximum corrosion currents in both

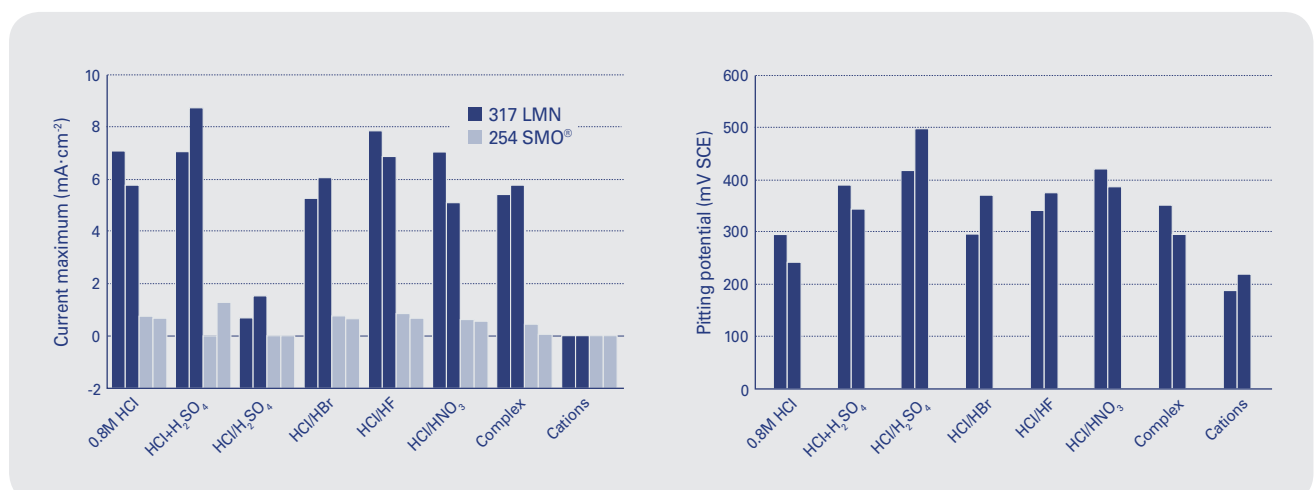
Fig. 6 Maximum current in polarisation curves in hydrochloric acid at different concentrations and temperatures. Shaded curves for 2507 indicate results when activation is used at the start of the potential scan. Without activation, or in deaerated conditions, the material is passive, as shown in the polarisation curves.



0.8M HCl and 1.6M HCl at 70°C which are shown by the shaded bars in Figure 6. Pitting corrosion was observed for 317 LMN in all five HCl environments, while the duplex steel 2205 exhibited pitting in 0.8M HCl and 1.6M HCl 70°C, and also showed some repassivating pitting at 50°C. This is in partial agreement with the alloy performance predicted from the empirical PRE relationship between pitting resistance and alloy composition, included in Table 3.

The effect of the presence of other ionic species is shown in Figure 7 for duplicate specimens of 317 LMN and 254 SMO[®]. Partial replacement of HCl by H₂SO₄ had a beneficial effect, causing 254 SMO[®] to passivate (as seen by the higher corrosion potential), decreasing the maximum current density for 317 LMN and also raising the pitting potential. Addition of sulphuric acid to the 0.8M HCl base solution induced passivation for one of the two specimens of 254 SMO[®] and increased the pitting potential for 317 LMN again indicating an inhibitive effect of sulphate. However, it also gave a minor increase in the corrosion rate of 317 LMN. The effect of sulphur is an interesting one in view of the high temperature sulphur effect discussed in §4.2. It means that sulphur additions made to mitigate high temperature chloride-induced corrosion can also have a beneficial downstream effect under acid condensation conditions. The disadvantages are

Fig. 7 Effect of additional species on the maximum current density in a base environment of 0.8M HCl at 70°C and on the pitting potential for 317 LMN. Environment designations according to Table 4.



that the presence of sulphur may cause condensation to commence at higher temperatures, also that the sulphur must naturally then be removed in the FGD system before reaching the stack, but multiple beneficial effects of a single addition nevertheless are an unexpected bonus.

Partial substitution of chloride by bromide, nitrate or fluoride had only a marginal influence on uniform corrosion, but nitrate increased the pitting potential for 317 LMN. Cation addition had a beneficial effect, causing both materials to shift to from active to passive behaviour because of the increase in redox potential, but also decreased the pitting potential for 317 LMN.

4.4 Comparison with field testing data

The field testing coupons were exposed in the pre-cooler of the waste-fired district heating plant, where the temperature was similar to that used in the laboratory tests. However, the gas had by that time undergone several cleaning steps subsequent to the position at which condensate was removed for analysis, so the environment is not identical. Results in terms of measured corrosion rates are given in Figure 9 show general trends in reasonable agreement with the laboratory evaluation, even though some differences are apparent. Corrosion rates are lower than those evaluated from that the measured peak current densities by roughly an order of magnitude. However, the peak current densities themselves are typically an order of magnitude higher than corrosion rates measured at the corrosion potential (e.g. by polarisation resistance measurements) so the agreement must be regarded as good. The relative ranking of the alloys is slightly different, and also differs between the two positions. At the top of the pre-cooler the highest corrosion rate is seen for 317 LMN, in agreement with the laboratory tests, while at the inlet the two duplex grades 2205 and 2507 have approximately three times the corrosion rate of 317 LMN.

Also included in Figure 8 are the maximum depths of pitting and crevice corrosion measured on the samples exposed at the top of the pre-cooler. Evaluation of the inlet specimens was not possible because of the high uniform corrosion rate of the duplex grades, particularly around the fusion line, Figure 9. The pitting ranking between the steel grades agrees with the observations from laboratory testing, with 317 LMN showing the largest pit depth, followed by 2205.

Fig. 8 Corrosion rates evaluated from test coupons exposed for 7 months in the pre-cooled of a waste-fired district heating plant, also maximum attack depths measured for specimens at the top of the pre-cooler.

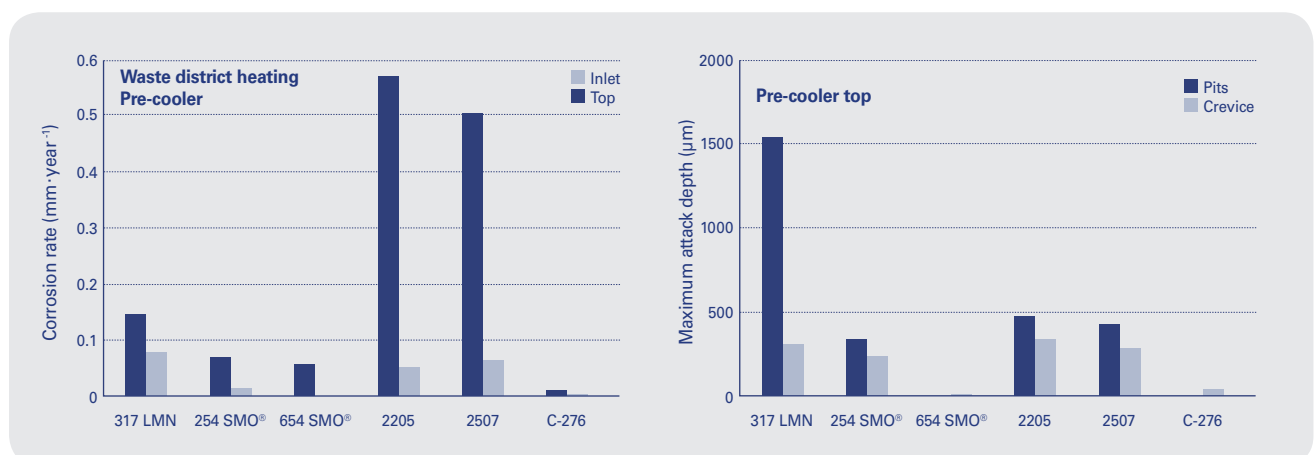


Fig. 9 Appearance of test panel after exposure for 7 months at the pre-cooler inlet and section of 2507 specimen showing corrosion in the fusion line.



4. Conclusions

The results obtained from the laboratory tests have shown that stainless steels provide attractive materials solutions in several stages of waste- or biomass-fired power plants. The high temperature austenitic stainless steel grades 253 MA[®] and 310S give very appreciable reduction in the corrosion rates under deposits compared with the widely-used low-alloy grade T22 (2Cr-1Mo). The benefit is often comparable with that for nickel-base alloys but at a significant cost advantage. Comparison with field tests provides evidence that the laboratory tests gave reasonably relevant corrosion rates, and confirmed the stainless steel advantages. These may be utilised in two ways, either giving an extension of component lifetimes or allowing an increase in process temperatures, and thus also plant energy efficiency.

In the lower temperature areas of the plant, acid condensation becomes an issue and stainless steels are often a necessary materials choice because lower alloyed materials simply do not have adequate corrosion resistance. An alternative may be polymers, but as soon as heat transfer is required for energy extraction, the heat conductivity of metallic materials becomes a necessity. Duplex stainless steels must be applied with care in the most aggressive condensation environments, because of the risk of selective corrosion, particularly around welds. However, particularly good results are seen for the superaustenitic grades 254 SMO[®] and 654 SMO[®], and the latter performs in many cases on a par with nickel-base alloys.

5. Acknowledgements

The laboratory testing in high temperature environments was carried out within the project Materials for increased performance in sustainable fuel combustion (BIOWAS) with a financial grant from the Research Fund for Coal and Steel of the European Community under contract no. RFS-CR-03020. The laboratory testing and field exposures was carried out within the project "Stainless steels for wet conditions in municipal incineration and combustion plants (Dewcor) with a financial grant from the Research Fund for Coal and Steel of the European Community under contract no 7210-PR/305.

6. References

- [1] Y. Kawahara: New weld overlay process and evaluation of corrosion-resistance in WTE boiler environments. *Corrosion Science* 44 (2002) 223–245
- [2] M. Spiegel: The role of salt melts on the corrosion of steels and nickel-base alloys in waste incineration plants. *Proc Conf. NACE Corrosion 99* Paper 337
- [3] M. Spiegel: Corrosion of 2.25Cr-1Mo and Alloy 625 beneath molten KCl-ZnCl₂. *Proc Conf. Eurocorr '99*,
- [4] M. K. Reser (editor) *Phase diagrams for ceramicists*, The American Ceramic Society, 1969
- [5] M. Linder, R. Gubner, U. Kivisäkk, J. Peultier, A. Bergquist, B. Beckers. R. Pettersson, J. Flyg. Report EUR 22082 EN "Stainless steels for wet conditions in municipal incineration and combustion plants" from the European Commission, RFCS Publications
- [6] Peter Szakálos, Rachel Pettersson, Pamela Henderson, Annika Stålenheim, Peter Sjövall, Mitigation of chloride-induced corrosion in waste and biomass-fired boilers. Consortium on Materials Engineering for Thermal Energy Processes, KME 308 (Elforsk, 2006)
- [7] P. Henderson, P. Szakálos, R. Pettersson, C. Andersson, J. Högberg: Reducing superheater corrosion in wood-fired boilers. *Materials and Corrosion* 57:2 (2006) 128–134
- [8] P. Viklund, R. Pettersson, A. Hjörnhede, P. Henderson, P. Sjövall: The effect of a sulphur-containing additive on the initial corrosion of superheater tubes in a waste-fired boiler *Eurocorr 2008*, 7–11 September, Edinburgh
- [9] R.F.A. Pettersson, J. Storesund, M. Nordling, Corrosion of overlay weld cladding in waterwalls of a waste-fired CFB boiler. *Eurocorr 2008*, 7–11 September, Edinburgh

Comments on acom and its articles or suggestions on future articles are appreciated and should be sent to the editor Jesper Gunnarsson at acom@outokumpu.com

Outokumpu is an international stainless steel company. Our vision is to be the undisputed number one in stainless, with success based on operational excellence. Customers in a wide range of industries use our stainless steel and services worldwide. We are dedicated to helping our customers gain competitive advantage.

OUTOKUMPU

Outokumpu Stainless AB, Avesta Research Centre
Box 74, SE-774 22 Avesta, Sweden
Tel. +46 (0) 226 - 810 00, Fax +46 (0) 226 - 810 77

www.outokumpu.com